Modeling of separation of fatty acid methyl esters derived from fisheries waste by urea complexation method

Hideo MARUYAMA*, Keito Fukuchi, Hideshi SEKI

Division of Marine Biosciences, Graduate School of Fisheries Sciences, Hokkaido University

Minato 3-1-1, Hakodate JAPAN, 041-8611

Telephone: +81-138-40-8813, Facsimile: +81-138-40-5048, E-mail: maruyama@fish.hokudai.ac.jp

* corresponding to the author

Abstract

The aim of the study is to develop a simulation model for the fractionation of fatty acid methyl esters (FAME).by urea complexation. The fatty acids (FAs) were obtained from squid liver and scallop mid-gut, which contain rich in eicosapentaenoic and docosahexaenoic acids well known as health-promoting FAs. FAs can be divided into saturated fatty acid (SFA), monounsaturated fatty acid (MFA), and polyunsaturated fatty acid (PFA) based on the number of double bond in their structure. A fractionation model is proposed and derived from the assumption of the urea-FAMEs complexation reactions, which included equilibrium constants (*K*) concerned with FAMEs-urea and urea-urea binding. The experiments were conducted at 5 and 28 °C. Different complexation behaviors were observed for SFAME, MFAME, and PFAME. The amount of SFAME captured in the urea inclusion body was larger than MFAME and PFAME. The urea-SFAME and urea-MFAME formation behavior agreed very well with the proposed model, but the urea-PFAME formation behavior showed a large error with the calculation results. The validation experiments showed that the relative error between the experimental data and the model prediction was within 15% for SFAME and MFAME.

KEYWORDS: Urea complexation; Fractionation; Fatty acid methyl ester; Polyunsaturated fatty acid; Saturated fatty acid; Biodiesel fuel

1. Introduction

From the perspective of environmental issues and the effective use of biomass resources, biodiesel production as an environmentally friendly fuel has received a great deal of attention over the past decade. Biodiesel is chemically a fatty acid methyl ester (FAME) and can be produced from animal fat, plant oil, or fish oil by reacting triglyceride with methanol in the presence of a catalyst. Various types of resources have been used in the production of biodiesel [1]. In about the last decade, there has been a growing interest in smart grids [2] for power generation using renewable energy sources [3] and for the construction of sustainable power grids [4]. Against this background, biodiesel production using microalgae has been attracting attention [5]. This reason is based on the fact that a large number of cells can be obtained in a short period time and also serve as a carbon dioxide fixer. The hormesis effect of the carbon source substances used in the culture has also been reported [6]. Furthermore, studies on the use of enzymes such as lipase in biodiesel production [5, 7, 8] and the conversion of glycerin, a byproduct, into high-value-added substances as raw materials [9], as well as reports on the determination of optimal conditions using optimization methods such as response surface methods and central composite programming [7], have also attracted attention.

On the other hand, it has been well known that fisheries wastes, especially viscera of fishes and shellfishes contain polyunsaturated fatty acid (PUFA), i.e., omega-3 fatty acids, docosahexaenoic acid (C22:6, DHA), and eicosapentaenoic acid (C20:5, EPA) [10]. EPA and DHA have been used in medicines and health supplements because they are well known to have health-promoting effects. The other fatty acids which are less actively available can be utilized as the resource of biodiesel if EPA and DHA could be separated in some methods. Unfortunately, fatty acids in fisheries waste have rarely been used as a resource of biodiesel.

Few studies have been reported in two decades. We are proceeding with the utilization of fisheries waste for biodiesel at present from the viewpoint of effective utilization of bio-resources.

Several separations and fractionation methods for triglycerides, fatty acids, and fatty acid alkyl ester have been proposed, for example, liquid-liquid extraction [11], chromatography [12,13], adsorption [14-17], urea complexation [18-24], winterization [25-29], and so on. Among them, the urea complexation method has been widely employed due to its easy operation, low costs, and low energy requirement. In this method, generally, the saturated fatty acid methyl esters (SFAME) are included in the solid phase and the polyunsaturated fatty acid methyl esters (PFAME) remained in the liquid phase [30]. This tendency is known to relate to the stability of the inclusion complex, and it has been reported that the stability of the urea inclusion body depends on the geometry of the molecules involved, and any deviation from a straight chain arrangement weakens the stability of the urea inclusion body [30]. In other words, the greatest advantage of this method is that SFAME and PFAME could be almost completely separated by this method, because they exist almost entirely in solid and liquid phases, respectively. However, the monounsaturated fatty acid methyl esters (MFAME) are ambiguously distributed in both phases.

The urea complexation method, using an urea inclusion body of urea and octyl alcohol, was discovered and patented in 1940 by Bengen [31]. Then, this technique has been used to separate fatty acids since the late 1940s, as an easy way and has been applied to several multiple separation processes. In addition, urea and metal ion complexes have been synthesized for use as fertilizers [32,33]. However, most of these studies on the urea complexation method were conducted under limited conditions, and the specific optimum conditions were determined only. It is very important to predict the degree of the fractionation by urea complexation for the design and optimal operation of the reaction system in industrial

applications from the viewpoint of chemical engineering. These predictions can be proposed by a model about urea complexation, and it is possible to predict the amount of urea required for the amount of FAME to be recovered in the separation process, and how much FAME will be fractionated into the solid and liquid phases. Although some studies have been reported that consider the phenomenon of urea complexation as phase equilibrium [34] or adsorption [35], there have not been a few studies about the estimation and prediction of fractionation of FAME using urea complexation.

In this study, we proposed the estimation model of FAME fractionation using the urea complexation method. The experiments were conducted with FAMEs derived from squid liver and scallop mid-gut at 5 and 28 °C. We only employed FAME derived from squid liver and scallop shell mid-gut, in particular, it has been reported that scallop mid-gut glands contain more EPA and DHA than other marine products [36,37]. Some parameters included in the proposed model could be determined by fitting of the data and a least squares regression. The proposed model was verified with some experiments with different conditions employed in the case of the determination of the model parameters. In this study, the model was validated using only FAMEs derived from squid liver and scallop mid-gut, and we did not employ commercial FAMEs. The applicability and the possibility of the proposed model will be discussed.

2. Materials and methods

2.1. Reagents and raw materials

Methanol, hexane, chloroform, toluene, urea, sodium sulfate, and p-dimethylaminobenzaldehyde (for urea determination) were purchased from Fujifilm Wako Pure Chemical Co. (Japan). Ethanol, diethyl ether, and hydrogen chloride-methanol (10 wt.%) solution were purchased from Kanto Chemical Co. Inc. (Japan). Methyl tricosanoate (internal standard for gas chromatography) was purchased from Sigma-Aldrich Japan Co. Inc. (Japan). All purchased reagents were used without further purification.

Japanese squids (*Todarodes pacificus*) were captured at Tsugaru Strait near Hakodate bay. Scallop mid-gut was supplied from Hakodate Plant of DOHSUI Co. Ltd. (Hokuto, Hokkaido prefecture, Japan). FAMEs have been prepared and derived from those raw materials, respectively.

2.2. Preparation of fatty acid methyl ester

The liver of squid and mid-gut of scallop were homogenized, and the lipids were extracted by Bligh and Layer method [38]. A desired amount of lipid was taken in a 100 mL bottle with a lid and dissolved in toluene. A certain amount of hydrogen chloride-methanol (10 wt.%) solution was added as a liquid catalyst for the esterification reaction. The bottle was set in a water bath and was heated at 90 °C for 120 minutes. After open cooling, fatty acid methyl esters were collected by liquid extraction using hexane and were stocked in a refrigerator (-20°C). The components of FAME were determined by gas chromatography (Shimadzu GC-2014, Japan) with an internal standard method using methyl tricosanoate (C23:0). Typical

GC chart spectra of FAMEs derived from squid liver are shown in Fig. 1. The components of fatty acid derived from squid liver and scallop mid-gut were summarized in Table 1. These profiles were almost the same as those reported in the literature [10,39].

2.3. Procedure of urea complexation experiment

A certain amount of FAME, urea, and ethanol (95 vol.%) were taken into a 25 mL cylindrical glass vessel with a lid. The vessel was set in a water bath at 65 °C for 60 minutes. Then, the vessel was set in a water bath (28 °C) or in a low-temperature room (5 °C) for 8 hours to deposit the urea-FAME complexes. The experimental conditions were summarized in Table 2. The ion strength and pH were not adjusted in all experiments. The initial concentration ranges of urea and FAMEs were 0.62-2.33 mol/L (urea), 0.16-0.65 mol/L (squid), and 0.17-0.51 mol/L (scallop), respectively. Most experiments were conducted twice.

After the deposition of urea-FAME complexes, the solid phase was separated from the liquid phase by the following procedure, which is shown in Fig. 2 as a flow chart.

The liquid phase was taken with a syringe with 0.45 μm filter carefully, and the mass of the taken liquid was measured by an electronic balance. 1 mL of the collected liquid was used to determine the amount of urea in the liquid phase, and the mass of the 1 mL of the collected liquid was measured for correction of the FAMEs amount in the liquid phase. Then the inside wall of the vessel and the surface of the solid phase were rinsed out with saturated urea ethanol solution and hexane, and then the rinsing solution was also taken with a syringe with 0.45 μm filter. The liquid phase was collected in 20 mL test tube with a lid. 2 mL of distilled water and 4 mL of hexane were added to the test tube. The vessel was shaken vigorously for 1 minute, then was left to stand for separating the aqueous and hexane phases. After this, the hexane phase (upper phase) was moved to 10 mL test tube with a lid. This operation was

repeated three times to collect hexane phase for measuring FAMEs.

After removing the liquid phase, the vessel was set in a heater (40 °C), and the solid phase was dried until the weight reach constant, and the dry weight of the solid was measured. The extraction procedure of FAMEs in the inclusion body is as follows. After drying, 4 mL of 0.1 M HCl solution was added to the cylindrical glass vessel with a lid to dissolve the solid phase. Then, 4 mL of hexane was added to the vessel, and the vessel was shaken vigorously for 1 minute. After this, the vessel was left to stand for separating the aqueous and hexane phases, then the hexane phase (upper phase) was moved to 10 mL test tube with a lid. This operation was repeated 3 times to extract whole FAMEs to the hexane phase. Hexane was evaporated by blowing nitrogen in a draft, and the extracted FAMEs were determined by GC after constant quantification. The urea concentration in the liquid phase was determined by a method proposed by Watt and Crisp (1954) [40]. The coloring reagent was prepared as follows: 0.2 g of p-dimethylaminobenzaldehyde was mixed with 1 mL of hydrochloric acid and 10 mL of 95 % (v/v) ethanol, and the mixture was stirred vigorously. 2 mL of the coloring reagent was added to 5 mL of the solution containing urea. At ten minutes after the addition, the absorbance value at a wavelength of 420 nm was measured using a spectrophotometer (Jasco V-630, JASCO co., Japan). The amount of urea in the solid phase was determined by subtracting the amount of urea in the liquid phase from the initial amount of urea. The error between the urea amount determined from this subtraction and the urea amount measured actually in the solid phase was within 3%.

Gas Chromatography was carried out using GC-2014 (Shimadzu, Japan), equipped with a frame ionization detector (FID) and a capillary column (Omegawax, 30 m × 0.32 μm × 0.25 mm film sickness, Supelco, USA). The column temperature was programmed from 140 ºC (5 min) to 200 ºC at 4 ºC/min and held 200 ºC for 50 min. The injector and the detector temperatures were 250 and 260 ºC, respectively. The carrier gas was helium used at a linear

velocity of 25 cm/s. The split ratio was 100:1. The mass of each component was determined by the internal standard method. Tricosanoic acid methyl ester (C23) was used as the internal standard. A_i and A_{C23} are defined as the area values of each component and C23, respectively, and w_i and w_{C23} are defined as the masses of each component and C23 in the injected sample. Since A_i and A_{C23} are determined from the analysis results and w_{C23} is a known value, the mass w_i of each component can be obtained from A_i w_{C23}/ A_{C23}. The composition of the FAMEs was determined by determining the mass of each component.

2.4. Urea complexation model

Based on the behavior of FAMEs in urea inclusion body (solid phase) already reported or obtained in this study, we considered this model as follows:

(1) FAMEs were divided into three categories, such as saturated FAME, monounsaturated MFAME, and polyunsaturated FAME.

(2) Each FAMEs could bind to urea to form urea inclusion body (solid phase).

(3) Inclusion bodies (solid phases) could be also formed by the binding of urea to each other.

(4) On binding and forming the urea inclusion body, the equilibrium relationships between the liquid and solid phases were assumed.

(5) A mass balance equation of urea in the solid phase in equilibrium could be considered.

(6) Substitute the solid-liquid equilibrium relationship into the mass balance equation.

(7) By fitting of the data to the model equation, the least-squares method was used to determine the model variables.

The dissolved species of urea in the liquid phase could be assumed to be associates (U_x) consists of x molecules of urea ($x \geq 1$). Some studies suggested that in solution, urea molecules formed a dimer or associates having a larger number of molecules [41,42]. Thus,

the following equilibrium relationship considered to be established in the liquid phase.

$$xU \leftrightarrow U_x \qquad ;(K_{as}) \tag{1}$$

x represents a stoichiometric coefficient. K_{as} is the equilibrium constant of Eq. (1). K_{as} is defined as follows.

$$K_{as} = \frac{C_{\mathrm{U}_x}}{C_{\mathrm{U}}{}^{x}} \tag{2}$$

Where, C_{U} and C_{U_x} represent the concentration of urea monomer and urea associate, respectively. The relationship between C_{U} and C_{U_x} could be expressed as follows.

$$C_{\mathrm{U}} = xC_{\mathrm{U}_x} \tag{3}$$

Assuming that the inclusion body of SFAME, MFAME, and PFAME are formed by independent reaction, these equilibrium relationships could be expressed as follows.

$$\mathrm{SFAME} + n_1U_x \leftrightarrow SU_{n_1x} \qquad ; (K_1) \tag{4}$$

$$\mathrm{MFAME} + n_2U_x \leftrightarrow MU_{n_2x} \qquad ; (K_2) \tag{5}$$

$$\mathrm{PFAME} + n_3U_x \leftrightarrow PU_{n_3x} \qquad ; (K_3) \tag{6}$$

Where, n_1, n_2, and n_3 represent the stoichiometric coefficient for U_x binding SFAME, MFAME, and PFAME, respectively. SU_{n1x}, MU_{n2x}, and PU_{n3x} represent the inclusion body for

SFAME, MFAME, and PFAME, respectively. The equilibrium constants in Eqs. (4)-(6) are defined as follows.

$$K_1 = \frac{C_{SU}}{C_S C_{U_x}^{\ n_1}} \tag{7}$$

$$K_2 = \frac{C_{MU}}{C_M C_{U_x}^{\ n_2}} \tag{8}$$

$$K_3 = \frac{C_{PU}}{C_P C_{U_x}^{\ n_3}} \tag{9}$$

Where, C_S, C_M, and C_P represent the equilibrium concentrations of SFAME, MFAME, and PFAME. C_{SU}, C_{MU}, and C_{PU} represent the mole of SU, MU, and PU in the inclusion body per unit mass. Expressing that the total molar amount of SFAME, MFAME, and PFAME are as N_{Si}, N_{Mi}, and N_{Pi}, therefore, the following equations are obtained.

$$N_{Si} = wC_{SU} + VC_S \tag{10}$$

$$N_{Mi} = wC_{MU} + VC_M \tag{11}$$

$$N_{Pi} = wC_{PU} + VC_P \tag{12}$$

Where V and w represent the liquid volume and the mass of the inclusion body at the equilibrium state in the system, respectively. By solving for C_S, C_M, and C_P in Eqs. (7)-(9), the following equations are obtained.

$$C_S = \frac{C_{SU}}{K_1 C_{U_x}^{\ n_1}} \tag{13}$$

$$C_{\mathrm{M}} = \frac{C_{\mathrm{MU}}}{K_2 C_{\mathrm{U}_x}^{\ n_2}} \tag{14}$$

$$C_{\mathrm{P}} = \frac{C_{\mathrm{PU}}}{K_3 C_{\mathrm{U}_x}^{\ n_3}} \tag{15}$$

By substituting C_{S}, C_{M}, and C_{P} expressed through Eqs. (13)-(15) to Eqs. (10)-(12), then solving for C_{SU}, C_{MU}, and C_{PU}, and using the relationships in Eq.(3), the following three equations are obtained.

$$wC_{\mathrm{SU}} = \frac{N_{\mathrm{Si}}}{1 + \dfrac{V}{wK_1 \left(C_{\mathrm{U}} / x\right)^{n_1}}} \tag{16}$$

$$wC_{\mathrm{MU}} = \frac{N_{\mathrm{Mi}}}{1 + \dfrac{V}{wK_2 \left(C_{\mathrm{U}} / x\right)^{n_2}}} \tag{17}$$

$$wC_{\mathrm{PU}} = \frac{N_{\mathrm{Pi}}}{1 + \dfrac{V}{wK_3 \left(C_{\mathrm{U}} / x\right)^{n_3}}} \tag{18}$$

Urea molecules was considered to form inclusion bodies (associates) in the absence of FAMEs. When '*m*' urea molecules form associates, U_x, in the liquid phase come together to form the solid phase, U_{mx}, the equilibrium relationship can be expressed as follows.

$$mU_x \leftrightarrow U_{mx} \qquad ; (K_4) \tag{19}$$

The equilibrium constant of the reaction expressed by Eq. (19), K_4, can be defined as follows.

$$K_4 = \frac{C_{\mathrm{U}_{mx}}}{C_{\mathrm{U}_x}^{\ m}} \tag{20}$$

$C_{\mathrm{U}_{mx}}$ represents a mole of U_{mx} in the unit mass of inclusion body. The total molar amount of urea in the system, $N_{\mathrm{U_S}}$, can be expressed as follows.

$$N_{\mathrm{U_S}} = n_1 x w C_{\mathrm{SU}} + n_2 x w C_{\mathrm{MU}} + n_3 x w C_{\mathrm{PU}} + w C_{\mathrm{U}_{mx}} \tag{21}$$

By substituting wC_{SU}, wC_{MU}, and wC_{PU} expressed through Eqs. (16)-(18) and $C_{\mathrm{U}_{mx}}$ obtained from Eq. (20) to Eq. (21), the following equation can be obtained as.

$$N_{\mathrm{U_S}} = n_1 x \frac{\dfrac{N_{\mathrm{Si}}}{V}}{1 + \dfrac{1}{wK_1 \left(C_{\mathrm{U}} / x\right)^{n_1}}} + n_2 x \frac{\dfrac{N_{\mathrm{Mi}}}{V}}{1 + \dfrac{1}{wK_2 \left(C_{\mathrm{U}} / x\right)^{n_2}}} + n_3 x \frac{\dfrac{N_{\mathrm{Pi}}}{V}}{1 + \dfrac{1}{wK_3 \left(C_{\mathrm{U}} / x\right)^{n_3}}} + wK_4 \left(\frac{C_{\mathrm{U}}}{x}\right)^m \tag{22}$$

In Eq. (22), N_{Si}, N_{Mi}, and N_{Mi} are given as the initial conditions, and $N_{\mathrm{U_S}}$, C_{SU}, C_{MU}, C_{PU}, w, and V can be determined experimentally. By fitting of the data to Eq. (22), the parameters x, n_1, n_2, n_3, m, K_1, K_2, K_3, and K_4 can be estimated by least-squares regressions using spread-sheet software.

3. **Results and Discussion**

3.1. Influence of initial dose of urea on amount of FAME captured in solid phase

The urea complexation experiments were conducted by varying the volume of the system, temperature, and initial doses of FAME and urea. Typical results were shown in Figs. 3-6. The experimental conditions were summarized in Table 2. In all results, the amount of FAME included in the urea inclusion body was significantly different from each other for SFAME, MFAME, and PFAME. This tendency corresponds to some previous studies reported [18-20,43-46]. The ordinate in these figures is expressed as mol, which is calculated using the average molecular weight determined from the component compositions of FAMEs derived from squid liver and scallop mid-gut (Table 1). The average molecular weights of FAMEs derived from squid liver and scallop mid-gut are calculated as 305.1 and 296.2 g/mol, respectively. As seen in Figs. 3-6, SFAME was the most frequently included, and MFAME also linearly increased in the amount included with increasing initial urea concentration. PFAME was rarely included. Salimon et al. (2012) conducted urea complexation experiments with various ratios of urea addition to the amount of fatty acids (FAs) mixture derived from seed oil added to the experimental system to the amount of oil added to the mixture [43]. In this study, it was reported that more than 90% of the SFAME was included even under the lowest urea condition, and the percentage of monounsaturated FA included increased from 60% to 90% with increasing urea. This result showed almost the same tendency as the results obtained in this study. Since the distribution of SFAME, MFAME, and PFAME to the solid phase of urea shows a unique tendency, we considered that there would be differences in the ability of SFAME, MFAME, and PFAME to form inclusion bodies.

Fig. 7 shows the relationship between the initial urea concentration, C_{Ui}, and the mass of

the solid phase (the inclusion body) at the equilibrium state. As seen in Figs. 7a and 7c, the mass of the inclusion body increased with increasing the dose of FAMEs and C_{Ui} at 28 °C. However, in the case of 5 °C, the mass of the inclusion body was not significantly related to the dose of FAMEs but increased with increasing C_{Ui}. Fig. 8 shows the relationship between C_{Ui} and the equilibrium urea concentration, C_U. In this case, the FAME dose was 0.25 g, C_U increased with increasing C_{Ui}, however, in the case of other doses, C_U was not varied too much. All values of C_U in the experimental range were lower than the saturation concentration [47]. In the next section, we will propose an urea-FAMEs complexation model and the quantitative discussion will be made about the complexation mechanism based on the model.

3.2 Verification of complexation model

Figs. 9-11 show the comparison of the experimental results shown in Figs. 3-7 and the values calculated from Eq. (31). In Figs. 9-11, the abscissa corresponds to the values that can be calculated using only the experimental values, and the ordinate corresponds to the values that can be calculated using both the experimental values and the model variables. This relationship expressed as Eqs. (16)-(18) for FAMEs. The parameters used in this calculation were summarized in Table 3. The correlation coefficient, r, in determining model parameter was summarized in Table 4. The initial experimental conditions were described in the captions of Figs. 9-11. As seen in Figs. 9-11, good agreements were confirmed as to SU, MU, and urea associate formation behavior with the proposed model. On the other hand, significant scatters were observed for PU formation. Eq. (22) was based on the mass balance in the solid phase. In addition, the amount of PFAME captured in the inclusion body was lesser than 5 % of the initially added amount of PFAME. We considered that many scatters in Figs. 9-11 may be due to the analytical errors in the measurement of the PFAME, which appear in small amounts in

the solid phase.

In Table 3, in the case of FAMEs derived from squid liver, the values of $K_{1\text{-}4}$ at 5°C were larger than those for 28°C. This reason is considered that the solubility of urea at 28°C is much higher than the solubility at 5°C. Based on the data shown in the literature [47], the solubility of urea is 61.4 g/L (1.02 mol/L) at 5°C and 111.7 g/L (1.86 mol/L) at 28°C.
Thus the amount of urea-FAMEs inclusion bodies or solid phase at 5°C should be larger than that at 28°C. However, the total urea concentrations shown in Fig. 6 did not exceed the saturation concentration at 5°C and 28°C. This suggests that the binding forces between urea and FAMEs at 5°C are also stronger than those at 28°C. The K_4 values for the FAMEs derived from squid and scallops at 28°C were not significantly different.

The relationship of the order of K values, $K_1 > K_2 > K_3$, reflects the experimental results well. The values of the parameters, x, n_1, n_2, m, K_1, K_2, and K_4 were almost the same values regardless of the origin of the FAMEs and the operating temperature. However, the values of n_3 (2.3 and 5.5) and K_3 (0.00267 and 0.199) were significantly different by the origin of FAMEs (squid liver and scallop mid-gut). The reason for the difference is considered to be complicated thus we cannot make it clear in this study. According to Table 1, the components of SFA (26.2 and 24.3), MFA (29.5 and 25.0), and PFA (33.4 and 40.2) in FAs derived from squid liver were different from those in FAs derived from scallop mid-gut. Especially the main components of PFA, EPA (10.2 and 22.7) and DHA (18.2 and 8.6), were quite different between the PFAs derived from squid liver lipid and scallop mid-gut. It can be considered that the differences in the component of EPA and DHA might affect the values of n_3 and K_3.

It has been reported that there is an approximate proportional relationship between the average number of urea added per carbon in a molecule for SFAME and MFAME, which are relatively easily taken into the solid phase by the urea complexation. A comparison of the literature values with the results of this study may be useful to verify the experimental results

of this study. Asahara (1950) has carried out urea complexation experiments using FAME (C6-C20, including saturated and unsaturated FAME). He attempted several combinations of FAME for urea complexation experiments and has reported that the ratio of FAME and urea molecule was increased with the number of carbon atoms in FAMEs [20]. The ratio corresponds to the average number of urea molecules binding to FAMEs molecules. Fig 12 shows the relationship between the urea/FAMEs molar ratio in the inclusion body (determined in this study and reported in the literature) and the number of carbon atoms in the FAMEs. The molar ratio determined in this study was slightly larger than those reported in the literature [18-20]. This reason was considered that we used the average carbon number and the average molecular weight of SFAME and MFAME in the calculation. However, the tendency of the increase in the molar ratio of urea/FAMEs showed almost the same tendency reported in the literature.

We conducted additional experiments to evaluate the validity of the proposed model. The experimental conditions were as follows: FAME derived from squid liver and scallop mid-gut 0.1 g; liquid volume 10 mL; C_{Ui} : 1.33 and 2.33 mol/L; the complexation (cooling) temperature: 5 and 28°C. Fig. 13 shows the comparison between the calculated values and the data of additional experiments except for the data used in the parameter determination. The solid, dashed, and dotted lines represent the values predicted by the proposed model with the parameters listed in Table 3. It can be recognized that the experimental and calculated values agreed except for PFAME (Fig. 13b). The relative error between the data and the model prediction values was within 15% for SFAME and MFAME.

Several separation methods of FAMEs have been proposed, in particular, separation or concentration methods of PFAMEs have been also proposed, such as supercritical fluid separation, molecular distillation, and so on [48,49]. Among them, the urea complexation method could be considered as the most effective method, because PFAMEs could be

separated from SFAME and MFAME very simply by a non-expensive and low-energy required process. By the urea complexation method, PFAMEs are concentrated almost exclusively in the liquid phase, while SFAMEs and MFAMEs are concentrated almost exclusively in the solid phase. Since both phases are a mixture of FAMEs and urea, it is necessary to refine FAMEs from the liquid or solid phase. The urea complexation method requires a purification process in its downstream process, and improving the efficiency of this refinery process will be a future problem.

Fig. 14 shows a schematic drawing of a general process flow of FAMEs separation including urea complexation. The proposed model can contribute determination of the amount of urea required for urea inclusion body formation and the amount of SFAME and MFAME in the solid phase (the urea inclusion body), as a result, which can also predict the amount of solvent required in the subsequent urea separation process, which may contribute to save energy and costs. From a practical viewpoint, studies about the combination of the urea complexation method with gel chromatography for the concentration and subsequent purification of the target FAME [50], and about the urea inclusion method using green solvents [51], have been reported in recent years. Future studies on the purification process after urea complexation would be paid attention to.

4. Conclusions

Recovery of fatty acid methyl esters (FAMEs) by entrapping in urea-FAMEs associate or inclusion body was investigated using fatty acids derived from squid liver and scallop mid-gut gland. We attempted to formulate the urea complexation reactions between FAMEs and urea, and verified the model with the experimental results. By dividing the FAMEs into three categories, they are saturated fatty acid (SFAME), monounsaturated fatty acid (MFAME), and polyunsaturated fatty acid (PFAME), and analyzing the experimental results with the proposed model, it was considered that the behavior of the urea complexation could be promoted to understand comprehensively.

The equilibrium constants of the complexation reactions between FAMEs and urea, and between urea and urea were determined by fitting the experimental results to the model with the least-squares method. The amount of SFAME and MFAME in the inclusion body was relatively well predicted by the model. However, the error between the calculated and experimental values of PFAME tended to be large due to fundamentally very small quantity of PFAME in the inclusion body. The order of magnitude of K values and n values for FAMEs derived from squid liver and scallop mid-gut are $K_1 > K_2 > K_3$ and $n_1 \cong n_2 > n_3$, respectively. These orders of K and n reflect the experimental results well for both complexation temperatures (5 and 28°C) as shown in Table 3. The ratio of K_1 and K_2, and K_1 and K_3 were 3.29 and 3.97×10^4 for squid FAMEs and 4.42 and 4.93×10^2 for scallop FAMEs, respectively at 28ºC. The binding strength between SFAME and urea molecules was considered to be greatest in FAMEs. The binding numbers of associated urea (n_1, n_2, n_3) were averagely estimated as 5.84, 6.44, and 2.3 for squid FAMEs, and 5.34, 6.04, and 5.5 for scallop FAMEs. As just described, the binding strength could be compared numerically as the equilibrium constant.

In a further study, it is necessary to investigate whether the model proposed in this study can predict the amount of FAMEs in the inclusion body using the FAMEs of different FA compositions. It is also necessary to examine how the model parameters are affected by the experimental results obtained from samples with the same molecular species of constituent FAMEs but different compositions.

Acknowledgment

The authors gratefully appreciate Mrs. Risa Watanabe, Mrs. Kana Onishi, and Mr. Hiroki Hoshikawa, former students of Department of Marine Bioresources Chemistry, Faculty of Fisheries, Hokkaido University for his help and efforts in the experiments.

Nomenclature

C_M	= equilibrium concentration of MFAME in liquid phase	[mol/m^3]
C_{MU}	= equilibrium concentration of MFAME in solid phase	[mol/kg]
C_P	= equilibrium concentration of PFAME in liquid phase	[mol/m^3]
C_S	= equilibrium concentration of SFAME in liquid phase	[mol/m^3]
C_{SU}	= equilibrium concentration of SFAME in solid phase	[mol/kg]
C_{PU}	= equilibrium concentration of PFAME in solid phase	[mol/kg]
C_U	= equilibrium concentration of urea monomer in liquid phase	[mol/m^3]
C_{Ui}	= initial concentration of urea monomer in liquid phase	[mol/m^3]
C_{Ux}	= equilibrium concentration of associated urea in liquid phase	[mol/m^3]
$C_{U_{mx}}$	= equilibrium concentration of associated urea in solid phase	[mol/kg]
K_{as}	= equilibrium constant defined in Eq. (2)	[(mol/m^3)$^{1-x}$]
K_1	= equilibrium constant defined in Eq. (7)	[m$^{3+3n_1}$ /(kg $\cdot$ mol^{n_1})]
K_2	= equilibrium constant defined in Eq. (8)	[m$^{3+3n_2}$ /(kg $\cdot$ mol^{n_2})]
K_3	= equilibrium constant defined in Eq. (9)	[m$^{3+3n_3}$ /(kg $\cdot$ mol^{n_3})]
K_4	= equilibrium constant defined in Eq. (27)	[m^{3m} /(kg $\cdot$ mol^{m-1})]
m	= stoichiometric coefficient for associated urea binding /-associated urea	[-]
n_1	= stoichiometric coefficient for associated urea binding SFAME	[-]
n_2	= stoichiometric coefficient for associated urea binding MFAME	[-]
n_3	= stoichiometric coefficient for associated urea binding PFAME	[-]
N_{Si}	= total molar amount of SFAME in the system	[mol]
N_{Mi}	= total molar amount of MFAME in the system	[mol]
N_{Pi}	= total molar amount of PFAME in the system	[mol]

N_{U_S}	= total molar amount of urea in the system	[mol]
U	= urea monomer molecule	[-]
U_x	= associated urea molecule	[-]
V	= liquid volume at equilibrium in the system	[m^3]
V_i	= initial liquid volume at equilibrium in the system	[m^3]
w	= mass of inclusion body at equilibrium in the system	[kg]
x	= number of urea molecule in associated urea molecule	[-]

References

[1] F. Ma, M.A. Hanna, Biodiesel production: a review, Bioresour. Technol. 70(1) (1999) 1-15. https://doi.org/10.1016/S0960-8524(99)00025-5

[2] A.O. Ali, M.R. Elmarghany, M.M. Abdelsalam, M.N. Sabry, A.M. Hamed, Closed-loop home energy management system with renewable energy sources in a smart grid: A comprehensive review, J. Energy Storage 50 (2022) 104609. https://doi.org/10.1016/j.est.2022.104609

[3] A. Rahman, O. Farrok, M.M. Haque, Environmental impact of renewable energy source based electrical power plants: Solar, wind, hydroelectric, biomass, geothermal, tidal, ocean, and osmotic, Renew. Sust. Energ. Rev. 161 (2022) 112279. https://doi.org/10.1016/j.rser.2022.112279

[4] A.A. Kebede, T. Kalogiannis, J. Van Mierlo, M. Berecibar, A comprehensive review of stationary energy storage devices for large scale renewable energy sources grid integration, Renew. Sust. Energ. Rev. 159 (2022) 112213. https://doi.org/10.1016/j.rser.2022.112213

[5] G.F. Mota, I.G. de Sousa, A.L.B. de Oliveira, A.L.G. Cavalcante, K.S. Moreira, F.T.T. Cavalcante, J.E. da Silva Souza, Í.R. de Aguiar Falcão, T.G. Rocha, R.B.R. Valério, S.C.F. de Carvalho, F.S. Neto, J. de França Serpa, R.K.C. de Lima, M.C.M. de Souza, J.C.S. dos Santos, Biodiesel production from microalgae using lipase-based catalysts: Current challenges and prospects, Algal Res. 62 (2022) 102616. https://doi.org/10.1016/j.algal.2021.102616

[6] L. Tang, Y. Zhou, Y. Zhang, H. Sun, The role of energy source or substrate in microbial hormesis, Curr. Opin. Toxicol. 29 (2022) 10-18. https://doi.org/10.1016/j.cotox.2021.12.001

[7] K.S. Moreira, L.S. Moura Junior, R.R. Monteiro, A.L. de Oliveira, C.P. Valle, T.M. Freire, P. Fechine, M. de Souza, G. Fernandez-Lorente, J.M. Guisan, J. dos Santos, Optimization of the Production of Enzymatic Biodiesel from Residual Babassu Oil (*Orbignya* sp.) via RSM, Catalysts 10 (2020) 414. https://doi.org/10.3390/catal10040414

[8] R.R.C. Monteiro, S. Arana-Pe~na, T.N. da Rocha, L.P. Miranda, A. Berenguer-Murcia, P.W. Tardioli, J.C.S. dos Santos, R. Fernandez-Lafuente, Liquid lipase preparations designed for industrial production of biodiesel. Is it really an optimal solution?, Renew. Energy 164 (2021) 1566e1587. https://doi.org/10.1016/j.renene.2020.10.071

[9] P.J. Lima, R.M. da Silva, C.A. Neto, N.C. Gomes Silva, J.E. Souza, Y.L. Nunes, J.C. Sousa Dos Santos, An overview on the conversion of glycerol to value-added industrial products via chemical and biochemical routes, Biotechnol. Appl. Biochem. (2021) 1-25. https://doi.org/10.1002/bab.2098

[10] D. Igarashi, K. Hayashi, H. Kishimura, Positional distribution of DHA and EPA in phosphatidylcholine and phosphatidylethanolamine from different tissues of squids, J. Oleo Sci. 50 (2001) 729-734. https://doi.org/10.5650/jos.50.729

[11] M.L. Savaliya, B.D. Dhorajiya, B.Z. Dholakiya, Current trends in separation and purification of fatty acid methyl ester, Sep. Purif. Rev. 44(1) (2015) 24-40. https://doi.org/10.1080/15422119.2013.872126

[12] K. Kittirattanapiboon, K. Krisnangkura, Separation of acylglycerols, FAME and FFA in biodiesel by sizeexclusion chromatography, Eur. J. Lipid Sci. Technol. 110 (2008) 422-427. https://doi.org/10.1002/ejlt.200700164

[13] M. Dolowy, A. Pyka, Chromatographic Methods in the Separation of Long-Chain Mono- and Polyunsaturated Fatty Acids, J. Chem. (2015) 120830. https://doi.org/10.1155/2015/120830

[14] G Üstün, Separation of fatty acid methyl esters from tall oil by selective adsorption, J.

Am. Oil Chem.' Soc. 73(2) (1996) 203-210. https://doi.org/10.1007/BF02523896

[15] S. Özgül-Yücel, S. Türkay, Purification of FAME by rice hull ash adsorption, J. Am. Oil Chem.' Soc. 80 (2003) 373-376. https://doi.org/10.1007/s11746-003-0706-0

[16] S.M. Damasceno, V. Ferraz, D.L. Nelson, J.D. Fabris, Selective adsorption of fatty acid methyl esters onto a commercial melecular sieve or activated charcoal prepared from the *Acrocomia aculeata* cake remaining from press-extracting the fruit kernel oil, AIMS Energy 6(5) (2018) 801-809. https://doi.org/10.3934/energy.2018.5.801

[17] H. Maruyama, H. Seki, A. Furukawa, Adsorption behavior of methyl palmitate onto silica particle surface, Colloids Interface Sci. Commun. 44 (2021) 100468. https://doi.org/10.1016/j.colcom.2021.100468

[18] H. Schlenk, R.T. Holman, Separation and stabilization of fatty acids by urea complexes, J. Am. Chem. Soc. 72(11) (1950) 5001-5004. https://doi.org/10.1021/ja01167a048

[19] O. Redlich, C. M. Gable, A. K. Dunlop, and R. W. Millar, Addition Compounds of Urea and Organic Substances, J. Am. Chem. Soc. 72(9) (1950) 4153-4160. https://doi.org/10.1021/ja01165a087

[20] S. Asahara, Separation of fatty acids by urea additives, Bulletin of Institute of Industrial Science. University of Tokyo 5(5) (1953) 101-104. https://repository.dl.itc.u-tokyo.ac.jp/record/24338/files/sk005005002.pdf

[21] H. Mu, J. Jin, D. Xie, X. Zou, X. Wang, X. Wang, Q. Jin, Combined urea complexation and argentated silica gel column chromatography for concentration and separation of PUFAs from tuna oil: based on improved DPA level, J. Am. Oil Chem. Soc. 93 (2016) 1157-1167. https://doi.org/10.1007/s11746-016-2842-5

[22] X. Wang, W. Xiaohan, Y. Chen, W. Jin, Q. Jin, X. Wang, Enrichment of branched chain fatty acids from lanolin via urea complexation for infant formula use, LWT 117 (2020) 108627. https://doi.org/10.1016/j.lwt.2019.108627

[23] P. Thammapat, S. Siriamornpun, P. Raviyan, Concentration of eicosapentaenoic acid (EPA) and docosahexaenoic acid (DHA) of asian catfish oil by urea complexation: optimization of reaction conditions, Warasan Songkhla Nakharin 38 (2016) 163-170. https://doi.org/10.14456/sjst-psu.2016.22

[24] G.D. Rosabal, A. Rodríguez, E. Contreras, J. Viedma, M. Muñoz, M. Trigo, S.P. Aubourg, A. Espinosa, Concentration of EPA and DHA from refined salmon oil by optimizing the urea–fatty acid adduction reaction conditions using response surface methodology, Molecules 24(9) (2019) 1642-1654. https://doi.org/10.3390/molecules24091642

[25] D. Cunha, V. Crexi, L. Pinto, Winterization of fish oil with solvent, Food Sci. Technol. 29 (2009) 207-213. https://doi.org/10.1590/S0101-20612009000100032

[26] Á. Pérez, A. Casas, C.M. Fernández, M.J. Ramos, L. Rodríguez, Winterization of peanut biodiesel to improve the cold flow properties, Bioresour. Technol. 101(19) (2010) 7375-7381. https://doi.org/10.1016/j.biortech.2010.04.063

[27] L. Vázquez, C.C. Akoh, Concentration of stearidonic acid in free fatty acid and fatty acid ethyl ester forms from modified soybean oil by winterization, J. Am. Oil Chem’ Soc. 88(11) (2011) 1775-1785. https://doi.org/10.1007/s11746-011-1857-1

[28] R. Morales-Medina, G. De León, M. Munio, A. Guadix, E. Guadix, Mass transfer modeling of sardine oil polyunsaturated fatty acid (PUFA) concentration by low temperature crystallization, J. Food Eng. 183 (2016) 16-23. https://doi.org/10.1016/j.jfoodeng.2016.03.009

[29] M. Abe, H. Komatsu, K. Yamagiwa, H. Tajima, Effect of nonionic surfactants on the low temperature winterization separation of fatty acid methyl ester mixtures, Fuel 190 (2017) 351-358. https://doi.org/10.1016/j.fuel.2016.10.124

[30] L. Vázquez , E. Ortego, M. Corzo-Martínez, G. Reglero, C.F. Torres, Stearidonic acid concentration by urea complexation from echium oil, J. Oleo Sci. 67 (2018) 1091-1099.

https://doi.org/10.5650/jos.ess18025

[31] F. Bengen, Urea channel inclusion compounds. German Patent Application O.Z. 12438 (March 18, 1940): Technical Oil Mission Microfilm Reel 6, frames 263-270 (in Germany), and Reel 143, pages 135-139 (in English)

[32] M.J. Rahman, P. Bozadjiev, Y. Pelovski, Studies on the effects of some additives on the physicomechanical properties of urea-ammonium sulphate (UAS) pellets, Fertili. Res. 38 (1994) 89-93. https://doi.org/10.1007/BF00748768

[33] O.B. Ibrahim, Complexes of urea Mn(II), Fe(II), Co(II), and Cu(II) metal ions, Adv. Appl. Sci. Res., 3 (2012) 3522-3539.

[34] D.A. Setyawardhani, H. Sulistyo, W.B. Sediawan, M. Fahrurrozi, T. Ariyanto, Solid-liquid equilibrium for binary and ternary phases of saturated fatty acid-urea-alcohol in urea complexation, J. Chem. Eng. Data 64 (2019) 5066-5078. https://doi.org/10.1021/acs.jced.9b00113

[35] D.A. Setyawardhani, H. Sulistyo, W.B. Sediawan, M. Fahrurrozi, Adsorption of saturated fatty acid in urea complexation: kinetics and equilibrium studies, AIP Conf. Proc. 1931 (2018) 030013. https://doi.org/10.1063/1.5024072

[36] K. Hayashi, Eicosapentaenoic acid-rich triglycerides of scallop hematopanccreas, Nippon Suisan Gakkaishi 54 (1988) 1449. https://doi.org/10.2331/suisan.54.1449

[37] K. Sugimoto, R. Hosomi, K. Fukunaga, T. Shimono, S. Kanda, T. Nishiyama, M. Yoshida, T. Yoshioka, K. Takahashi, Genotoxicity evaluation of oil prepared from the internal organs of the Japanese giant scallop (Patinopecten yessoensis), Fundam. Toxicol. Sci. 6 (2019) 134-143. https://doi.org/10.2131/fts.6.137

[38] E.G. Bligh, W.J. Dyer, A rapid method of total lipid extraction and purification, Can. J. Biochem. Physiol. 37 (1959) 911-917. https://doi.org/10.1139/o59-099

[39] K. Hayashi, H. Kishimura, Seasonal changes in the contents of eicosapentaenoic acid

containing triglycerides in hepatopancreas of scallop, Nippon Suisan Gakkaishi 57(7) (1991) 1397-1401. https://doi.org/10.2331/suisan.57.1397

[40] G.W. Watt, J.D. Chrisp, Spectrophotometric method for determination of urea, Anal. Chem. 26 (1954) 452-453. https://doi.org/10.1021/ac60087a006

[41] C. Lee, E.A. Stahlberg, G. Fitzgerald, Chemical structure of urea in water, J. Phys. Chem. 99 (1995) 17737-17741. https://doi.org/10.1021/j100050a011

[42] F. Ramondo, L. Bencivenni, R. Caminiti, A. Pieretti, L. Gontrani, Dimerisation of urea in water solution: a quantum mechanical investigation, Phys. Chem. Chem. Phys. 9 (2007) 2206-2215. https://doi.org/10.1039/B617837E

[43] J. Salimon, B. Abdullah, N. Salih, Selectively increasing of polyunsaturated (18:2) and monounsaturated (18:1) fatty acids in Jatropha curcas seed oil by crystallization using D-optimal design, Chem. Cent. J. 6 (2012) 65. https://doi.org/10.1186/1752-153x-6-65

[44] M. Wu, H. Ding, S. Wang, S. Xu, Optimizing conditions for the purification of linoleic acid from sunflower oil by urea complex fractionation, J. Am. Oil Chem. Soc. 85 (2008) 677-684. http://doi.org/10.1007/s11746-008-1245-7

[45] B. Jiang, Y. Liu, L. Zhang, Y. Sun, Y. Liu, X. Liu, Study on the concentration of unsaturated fatty acid methyl esters by urea complexation, J. Chem. Soc. Pak. 36 (2014) 1013-1020.

[46] M.Á. Rincón-Cervera, R. Galleguillos-Fernández, V. González-Barriga, R. Valenzuela, A. Valenzuela, Concentration of gamma-linolenic and stearidonic acids as free fatty acids and ethyl esters from viper's bugloss seed oil by urea complexation, Eur. J. Lipid Sci. Technol. 120 (2018) 1800208. https://doi.org/10.1002/ejlt.201800208

[47] F. Lee, L.E. Lahti, Solubility of urea in water-alcohol mixtures, J. Chem. Eng. Data 17 (1972) 304-306. https://doi.org/10.1021/je60054a020

[48] N. Rubio-Rodríguez, S. Beltrán, I. Jaime, S.M. de Diego, M.T. Sanz, J.R. Carballido,

Production of omega-3 polyunsaturated fatty acid concentrates: A review, Innov. Food Sci. Emerg. Technol. 11 (2010) 1-12. https://doi.org/10.1016/j.ifset.2009.10.006

[49] M. Haq, A.T. Getachew, P.S. Saravana, Y.J. Cho, S.K. Park, M.J. Kim, B.S. Chun, Effects of process parameters on EPA and DHA concentrate production from Atlantic salmon by-product oil: Optimization and characterization. Korean J. Chem. Eng. 34 (2016) 2255-2264. https://doi.org/10.1007/s11814-016-0362-5

[50] H. Mu, J. Jin,; D. Xie, X. Zou, X. Wang, X. Wang, Q. Jin, Combined Urea Complexation and Argentated Silica Gel Column Chromatography for Concentration and Separation of PUFAs from Tuna Oil: Based on Improved DPA Level, J. Am. Oil Chem. Soc. 93 (2016) 1157-1167. https://doi.org/10.1007/s11746-016-2842-5

[51] L. Vázquez, M. Sánchez-Moyano, L. de la Iglesia, G. Reglero, C.F. Torres, A new urea adducts method for PUFA concentration using green food grade solvents and avoiding ethyl carbamate formation, Food Chem. 392 (2022) 133197. https://doi.org/10.1016/j.foodchem.2022.133197

Figures and Tables captions

Fig. 1. Typical gas chromatogram of fatty acid methyl esters derived from squid liver.

Fig. 2. Flow chart of procedure of determination of FAMEs and urea.

Fig. 3. The relationship between molar amount of FAMEs in urea inclusion body and the initial concentration of urea, C_{Ui}. Experimental conditions: the initial amount of FAME prepared from squid liver: (a) 0.25 g, (b) 0.5 g, (c) 0.75 g; the volume of solvent 5 mL; the complexation temperature 28ºC.

Fig. 4. The relationship between molar amount of FAMEs in urea inclusion body and the initial concentration of urea, C_{Ui}. Experimental conditions: the initial amount of FAMEs derived from squid liver: (a) 1.0 g, (b) 2.0 g ; the volume of solvent 10 mL; the complexation temperature 28ºC.

Fig. 5. The relationship between molar amount of FAMEs in urea inclusion body and the initial concentration of urea, C_{Ui}. Experimental conditions: the initial amount of FAMEs derived from squid liver: (a) 0.25 g, (b) 0.5 g, (c) 0.75 g ; the volume of solvent 5 mL; the complexation temperature 5 ºC.

Fig. 6. The relationship between molar amount of FAMEs in urea inclusion body and the initial concentration of urea, C_{Ui}. Experimental conditions: the initial amount of FAMEs derived from scallop mid-gut gland, (a) 0.25 g, (b) 0.5 g, (c) 0.75 g ; the volume of solvent 5 mL; the complexation temperature 28 ºC.

Fig. 7. Relationship between the mass of the solid phase (inclusion body), w, and the initial urea concentration, C_{Ui}. Kinds of FAMEs, the initial dose of FAMEs, the system volume and the complexation temperature were shown in figures.

Fig. 8. Relationship between the equilibrium urea concentration, C_U, and the initial urea

concentration, C_{Ui}. Kinds of FAMEs, the initial dose of FAMEs, the system volume and the complexation temperature were shown in figures.

Fig. 9. Fitting of the data shown in Figs. 3, 5, and 7 obtained with FAME derived from squid liver to Eqs. (16)-(18) and (22) for determination of the model parameters by least-squares regression. 5 or 10 mL of solvent volume (ethyl alcohol) and 28ºC as complexation temperature were employed in these experiments.

Fig. 10. Fitting of the data shown in Figs. 5 and 7 obtained with FAME derived from squid liver to Eqs. (16)-(18) and (22) for determination of model parameters by a least squares method. 5 mL of solvent volume (ethyl alcohol) and 5ºC as complexation temperature were employed in these experiments.

Fig. 11. Fitting of the data shown in Figs. 6 and 7 obtained by using FAME (scallop shell midgut) to Eqs. (16)-(18) and (22) for determination of model parameters by a least squares method. 5 mL of solvent volume (ethyl alcohol) and 28ºC as complexation temperature were employed in these experiments.

Fig. 12. Relationship of carbon number of fatty acid (FA) or FAME and number of urea binding to FA or FAME in the solid phase (urea inclusion body).

Fig. 13. Comparison between the molar amount of FAME in the solid phase (urea inclusion body) of the calculated (lines) and the experimental values (symbol) for (a) FAME derived from squid liver (28ºC), (b) FAME derived from squid liver (5ºC), and (c) FAME derived from scallop mid-gut (28ºC).

Fig. 14 Schematic diagram of process flow including urea complexation

Table 1 The contents of fatty acid derived from squid liver and scallop viscera.

Table 2 The experimental condition of Figs. 3-6.

Table 3 Model parameters determined from fitting of the data of Figs. 3-8 to Eq. (22) by a least squares method.

Table 4 Correlation coefficients, *r*, in determining model parameters by least squares method in Figs. 9-11.

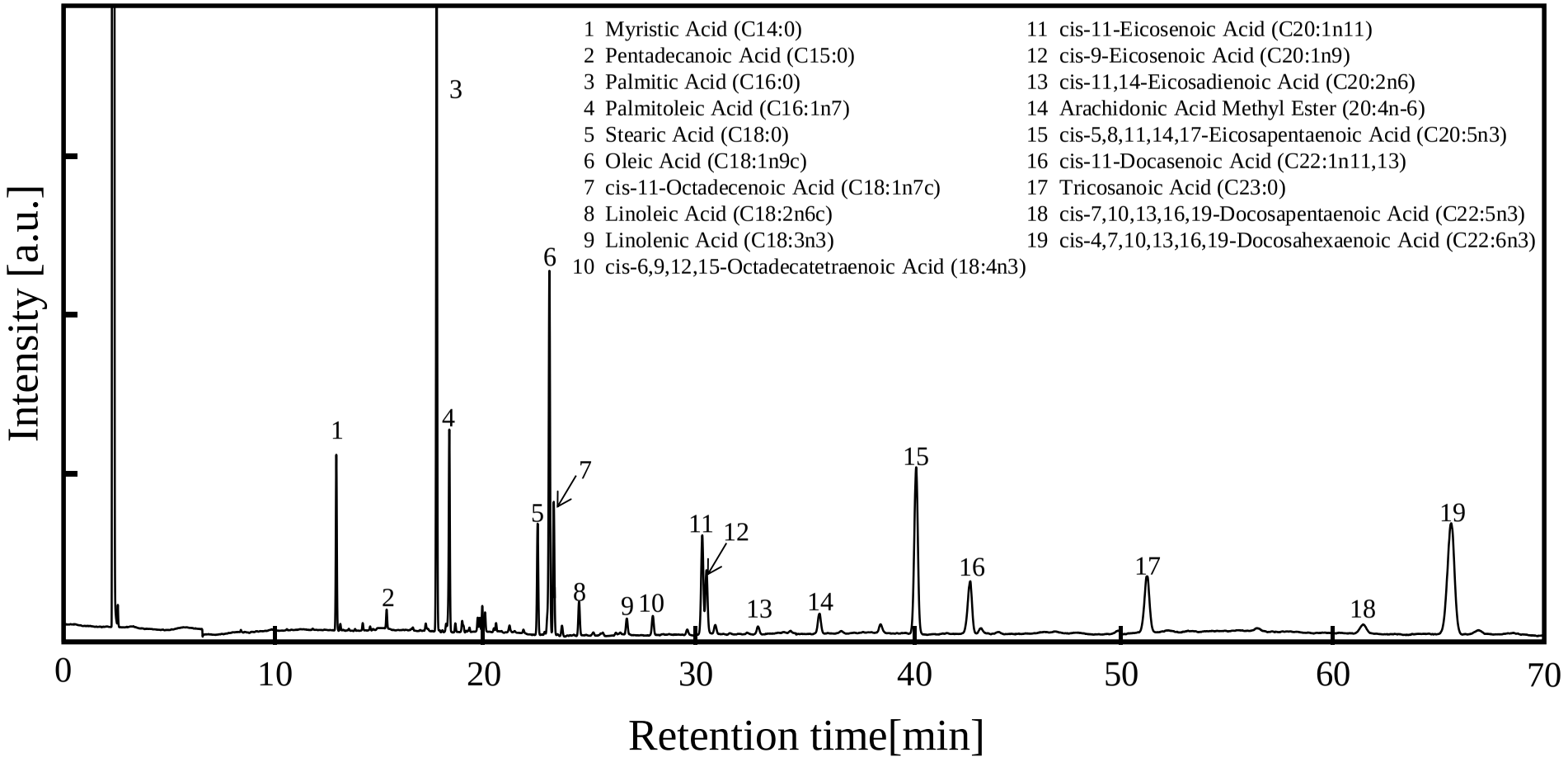

Fig. 1. Typical gas chromatogram of fatty acid methyl esters derived from squid liver.

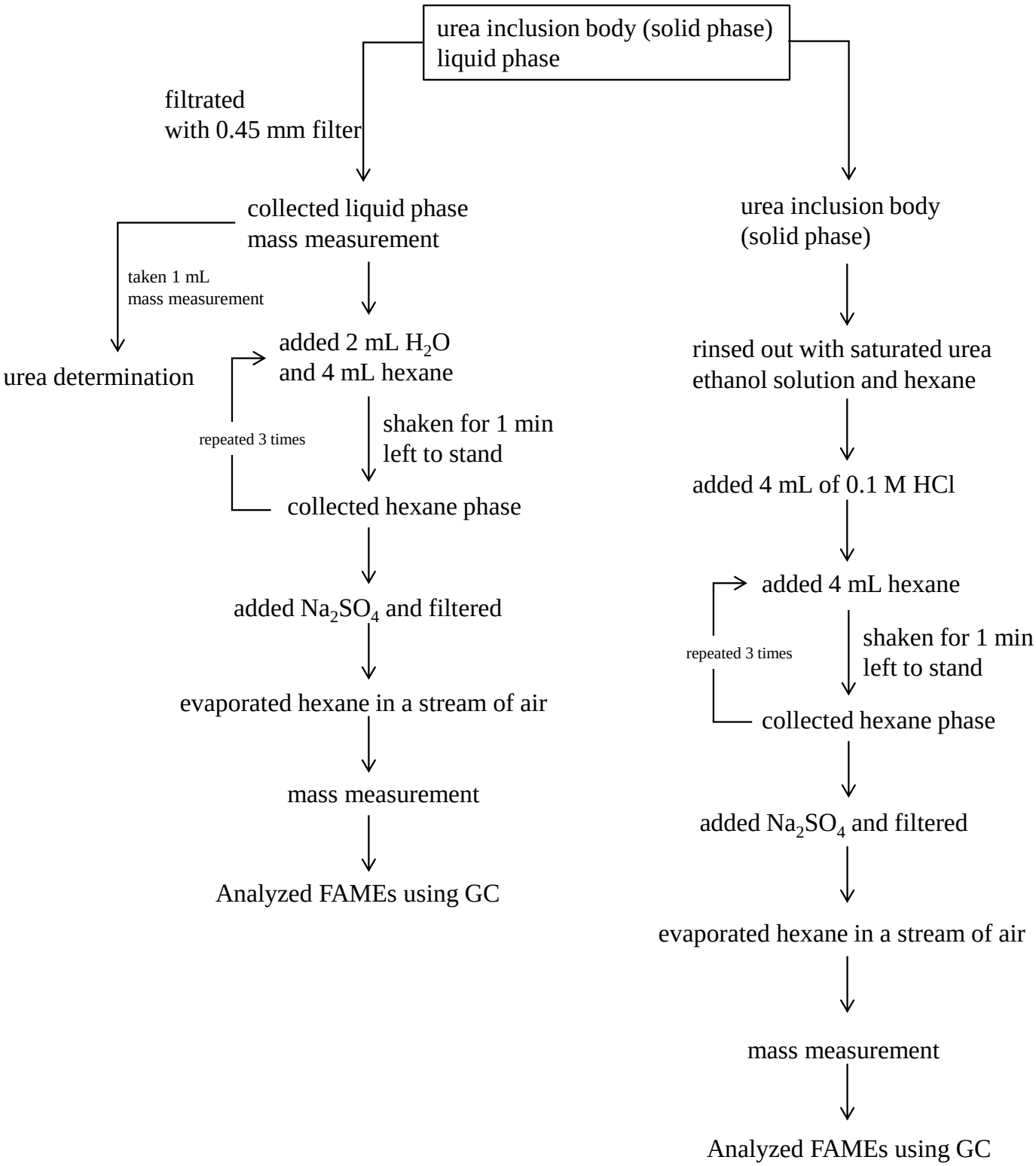

Fig. 2. Flow chart of procedure of determination of FAMEs and urea.

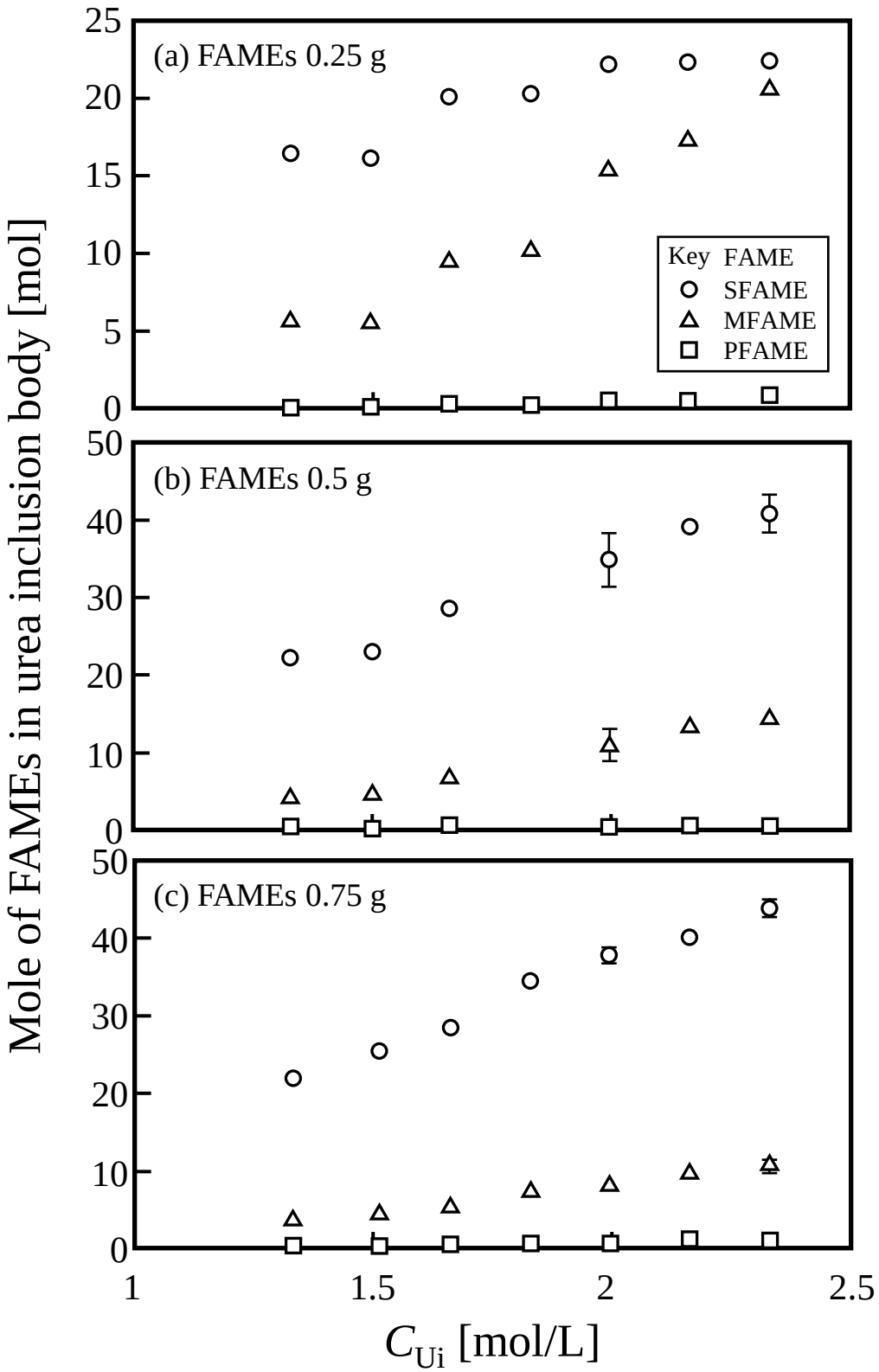

Fig. 3. The relationship between molar amount of FAMEs in urea inclusion body and the initial concentration of urea, C_{Ui}. Experimental conditions: the initial amount of FAME prepared from squid liver: (a) 0.25 g, (b) 0.5 g, (c) 0.75 g; the volume of solvent 5 mL; the complexation temperature 28ºC.

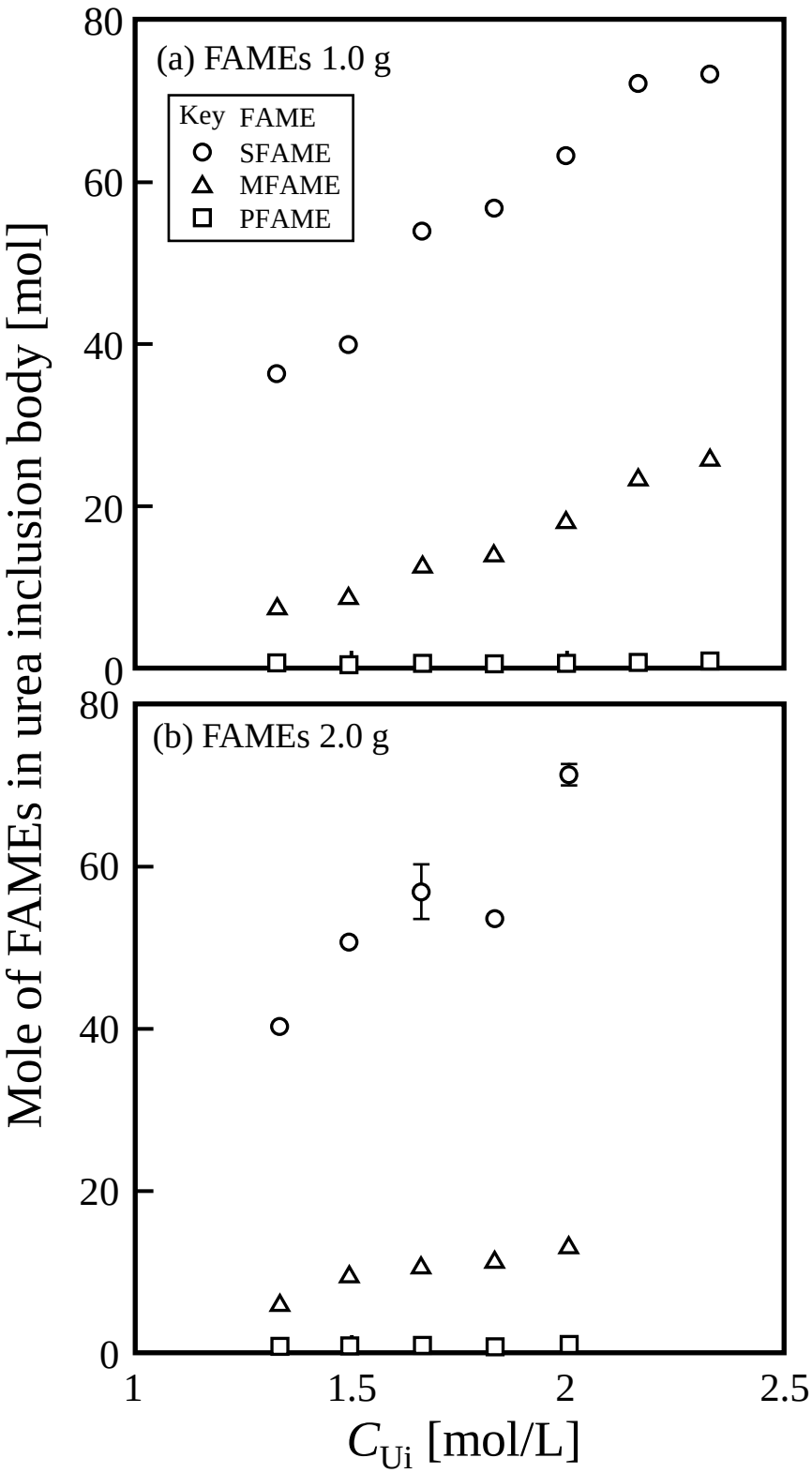

Fig. 4. The relationship between molar amount of FAMEs in urea inclusion body and the initial concentration of urea, C_{Ui}. Experimental conditions: the initial amount of FAMEs derived from squid liver: (a) 1.0 g, (b) 2.0 g ; the volume of solvent 10 mL; the complexation temperature 28ºC.

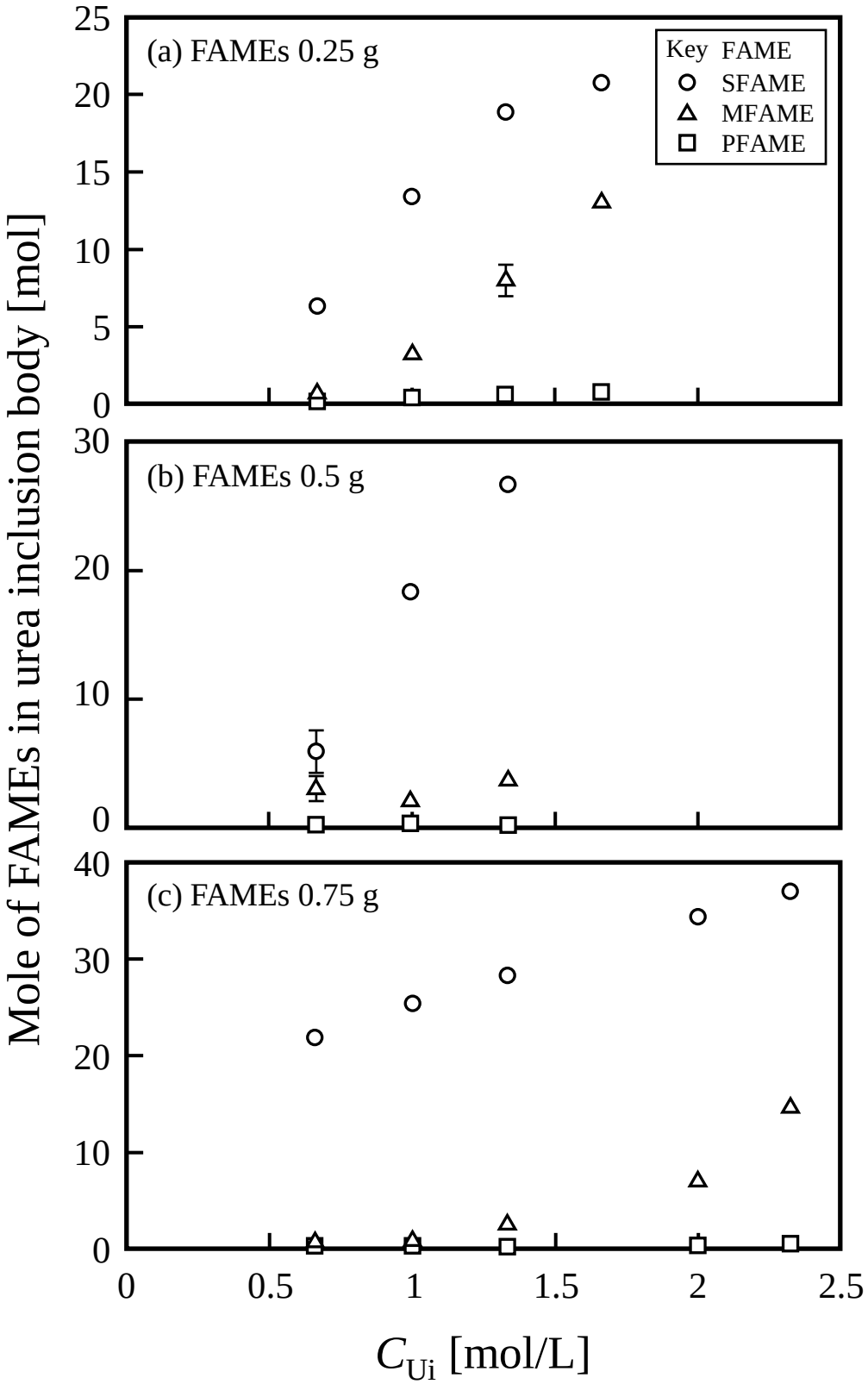

Fig. 5. The relationship between molar amount of FAMEs in urea inclusion body and the initial concentration of urea, C_{Ui}. Experimental conditions: the initial amount of FAMEs derived from squid liver: (a) 0.25 g, (b) 0.5 g, (c) 0.75 g ; the volume of solvent 5 mL; the complexation temperature 5 ºC.

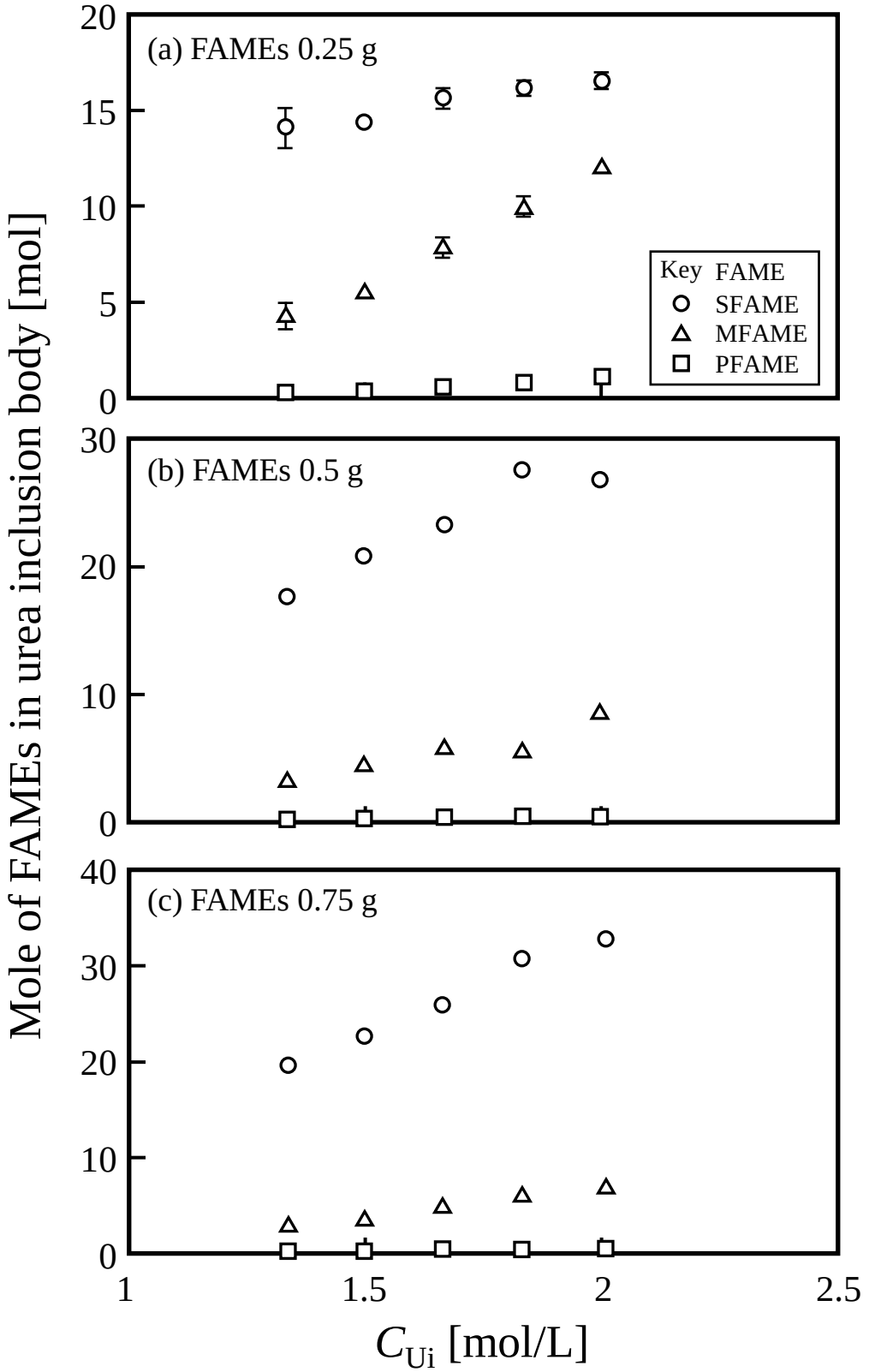

Fig. 6. The relationship between molar amount of FAMEs in urea inclusion body and the initial concentration of urea, C_{Ui}. Experimental conditions: the initial amount of FAMEs derived from scallop mid-gut gland, (a) 0.25 g, (b) 0.5 g, (c) 0.75 g ; the volume of solvent 5 mL; the complexation temperature 28 ºC.

Fig.5

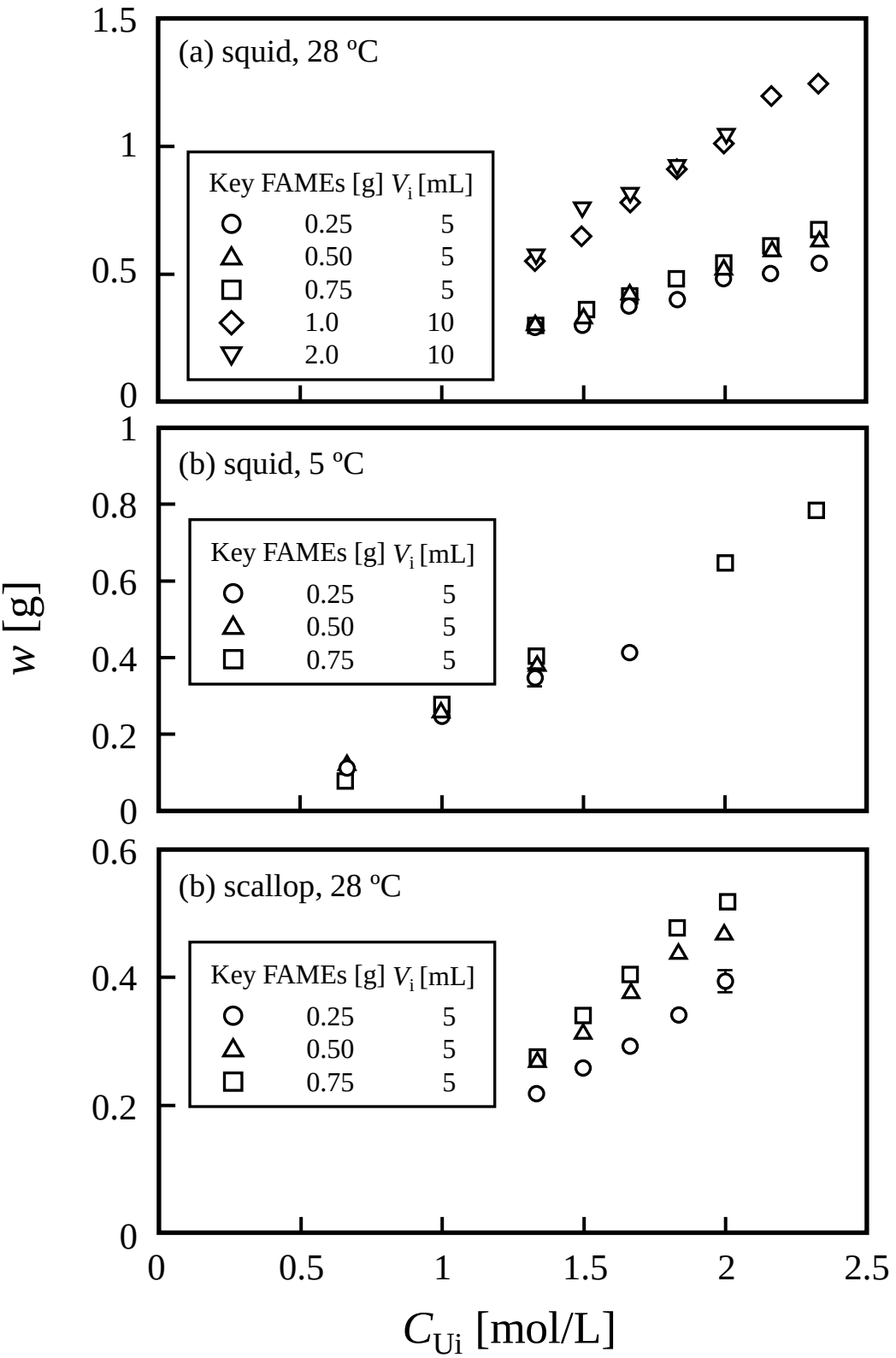

Fig. 7. Relationship between the mass of the solid phase (inclusion body), *w*, and the initial urea concentration, C_{Ui}. Kinds of FAMEs, the initial dose of FAMEs, the system volume and the complexation temperature were shown in figures.

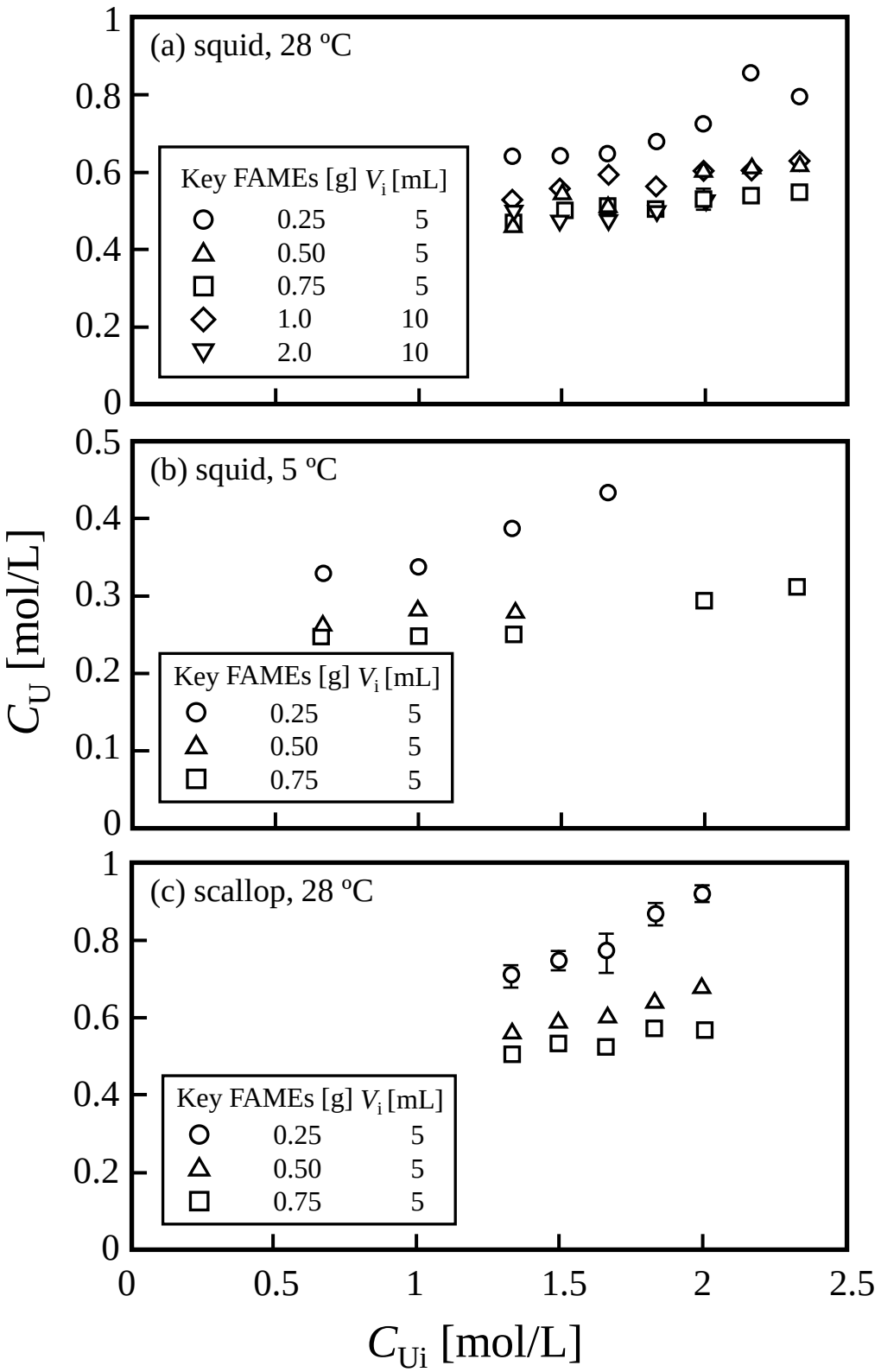

Fig. 8. Relationship between the equilibrium urea concentration, C_U, and the initial urea concentration, C_{Ui}. Kinds of FAMEs, the initial dose of FAMEs, the system volume and the complexation temperature were shown in figures.

Figure 7

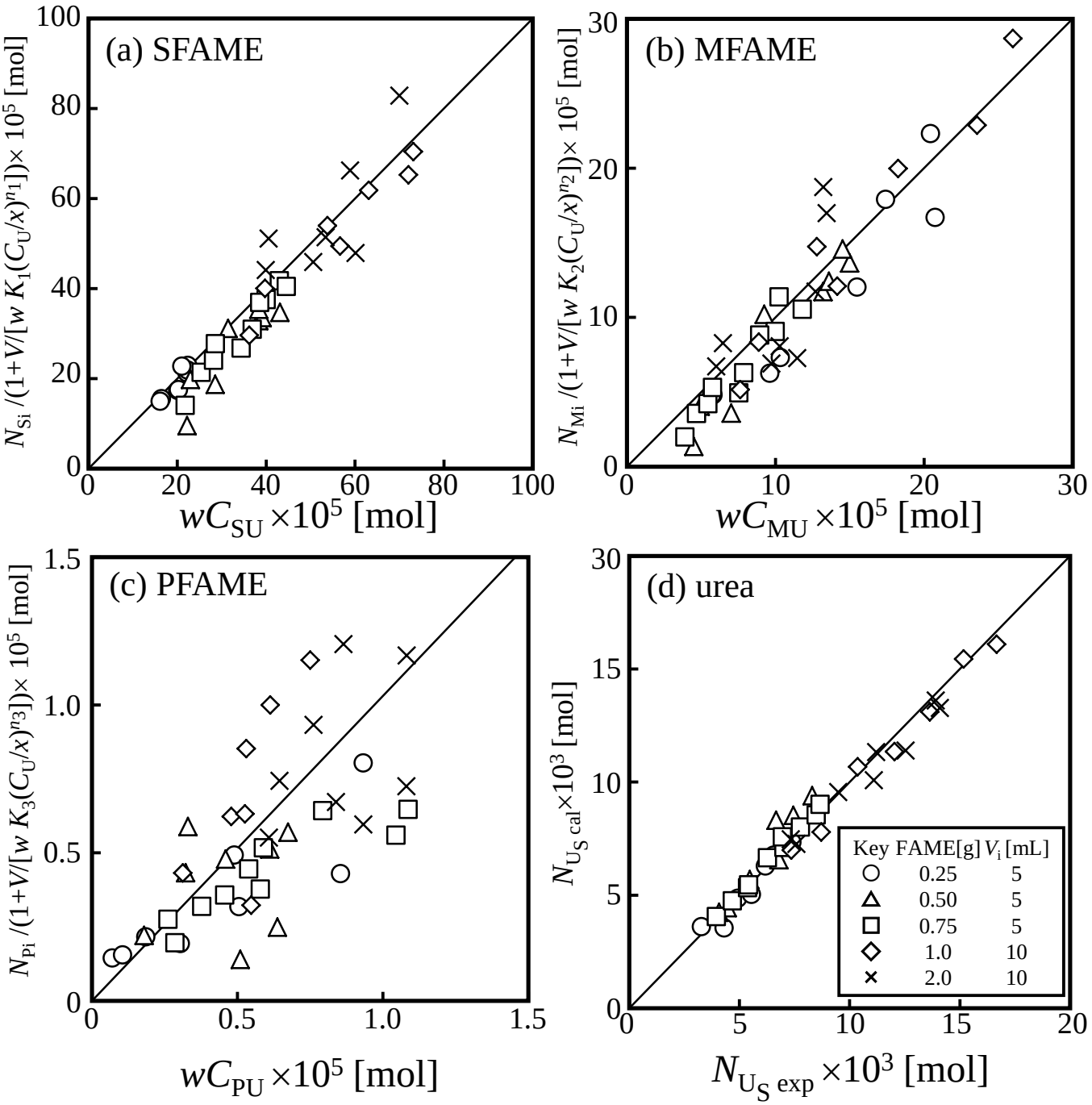

Fig. 9. Fitting of the data shown in Figs. 3, 5, and 7 obtained with FAME derived from squid liver to Eqs. (16)-(18) and (22) for determination of the model parameters by least-squares regression. 5 or 10 mL of solvent volume (ethyl alcohol) and 28ºC as complexation temperature were employed in these experiments.

Figure 8

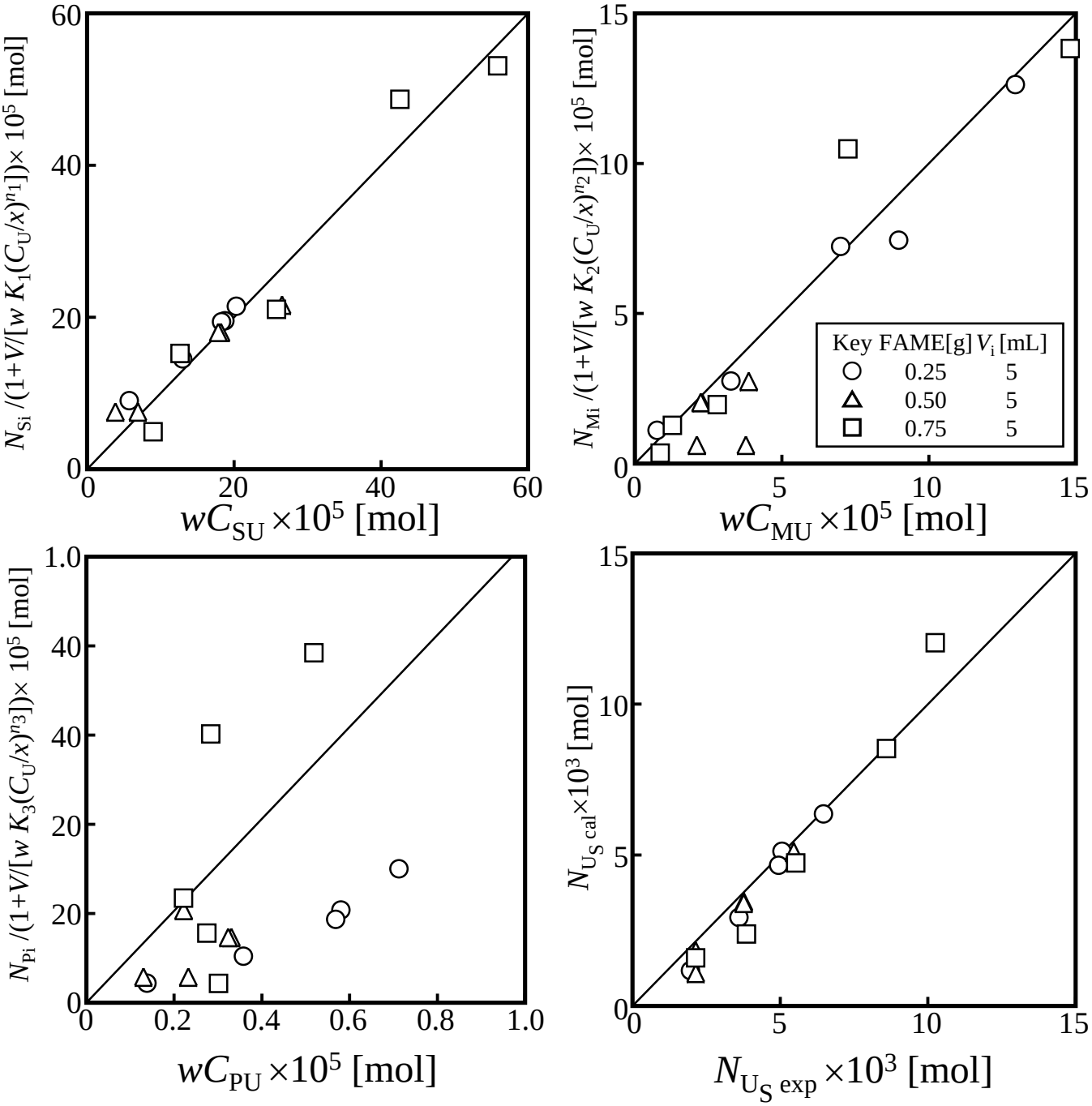

Fig. 10 Fitting of the data shown in Figs. 5 and 7 obtained with FAME derived from squid liver to Eqs. (16)-(18) and (22) for determination of model parameters by a least squares method. 5 mL of solvent volume (ethyl alcohol) and 5ºC as complexation temperature were employed in these experiments.

Figure 9

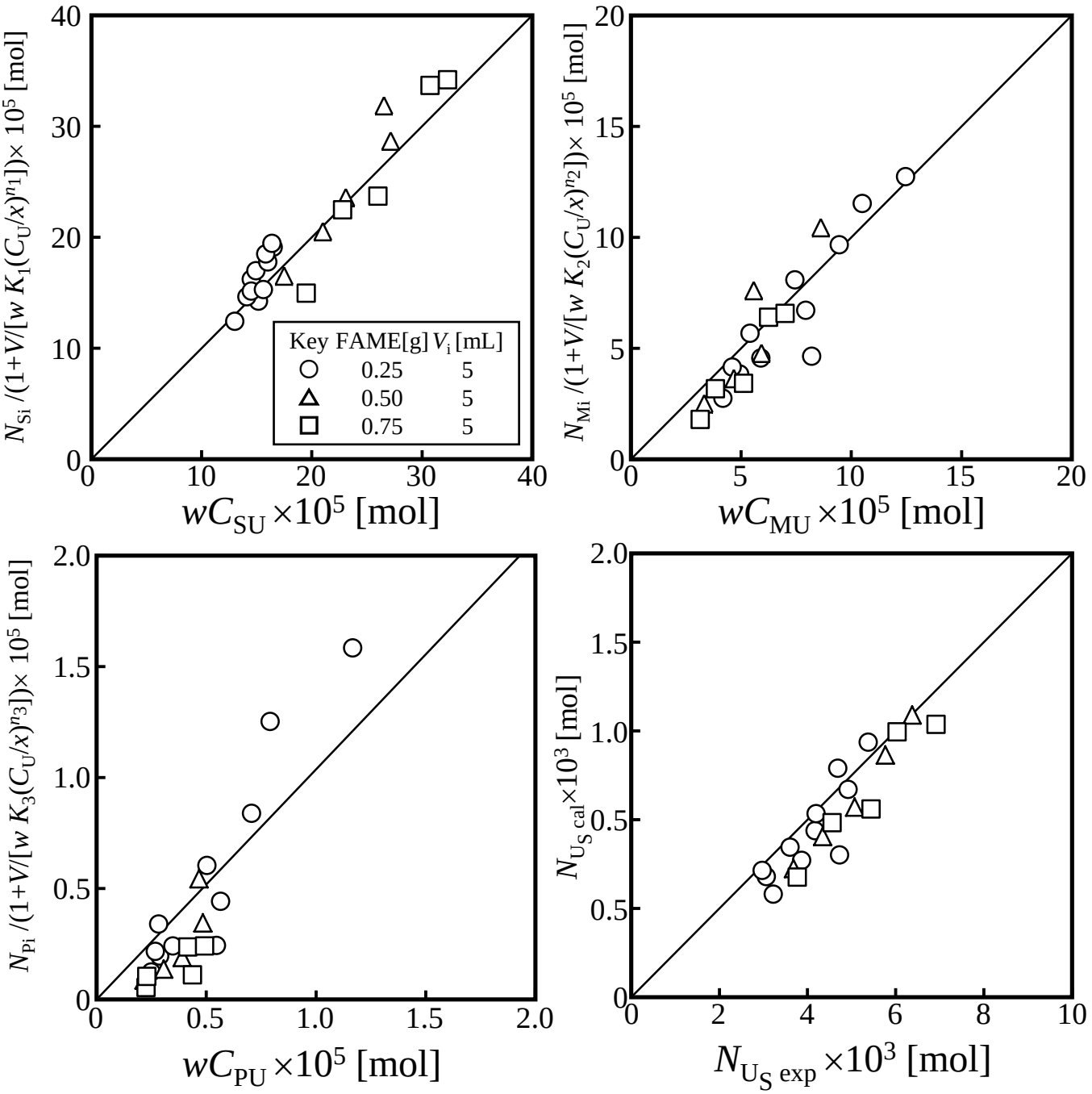

Fig. 11. Fitting of the data shown in Figs. 6 and 7 obtained by using FAME (scallop shell midgut) to Eqs. (16)-(18) and (22) for determination of model parameters by a least squares method. 5 mL of solvent volume (ethyl alcohol) and 28ºC as complexation temperature were employed in these experiments.

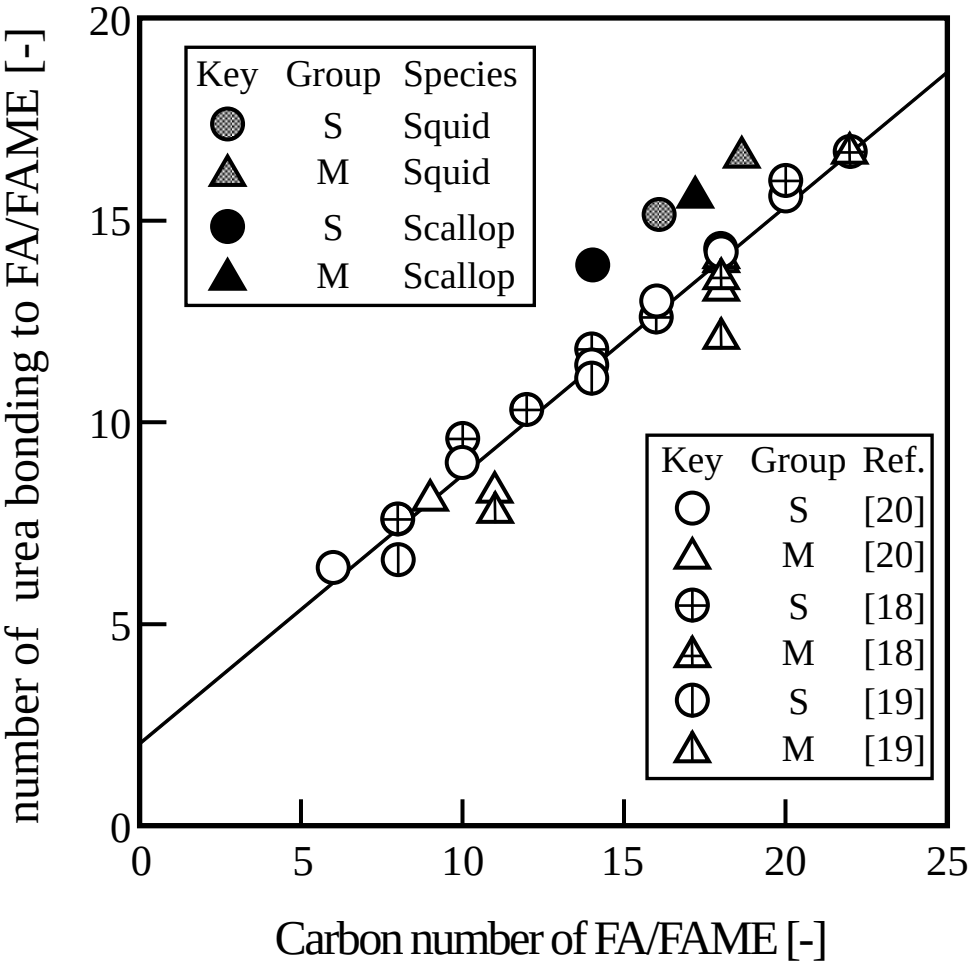

Fig. 12. Relationship of carbon number of fatty acid (FA) or FAME and number of urea binding to FA or FAME in the solid phase (urea inclusion body).

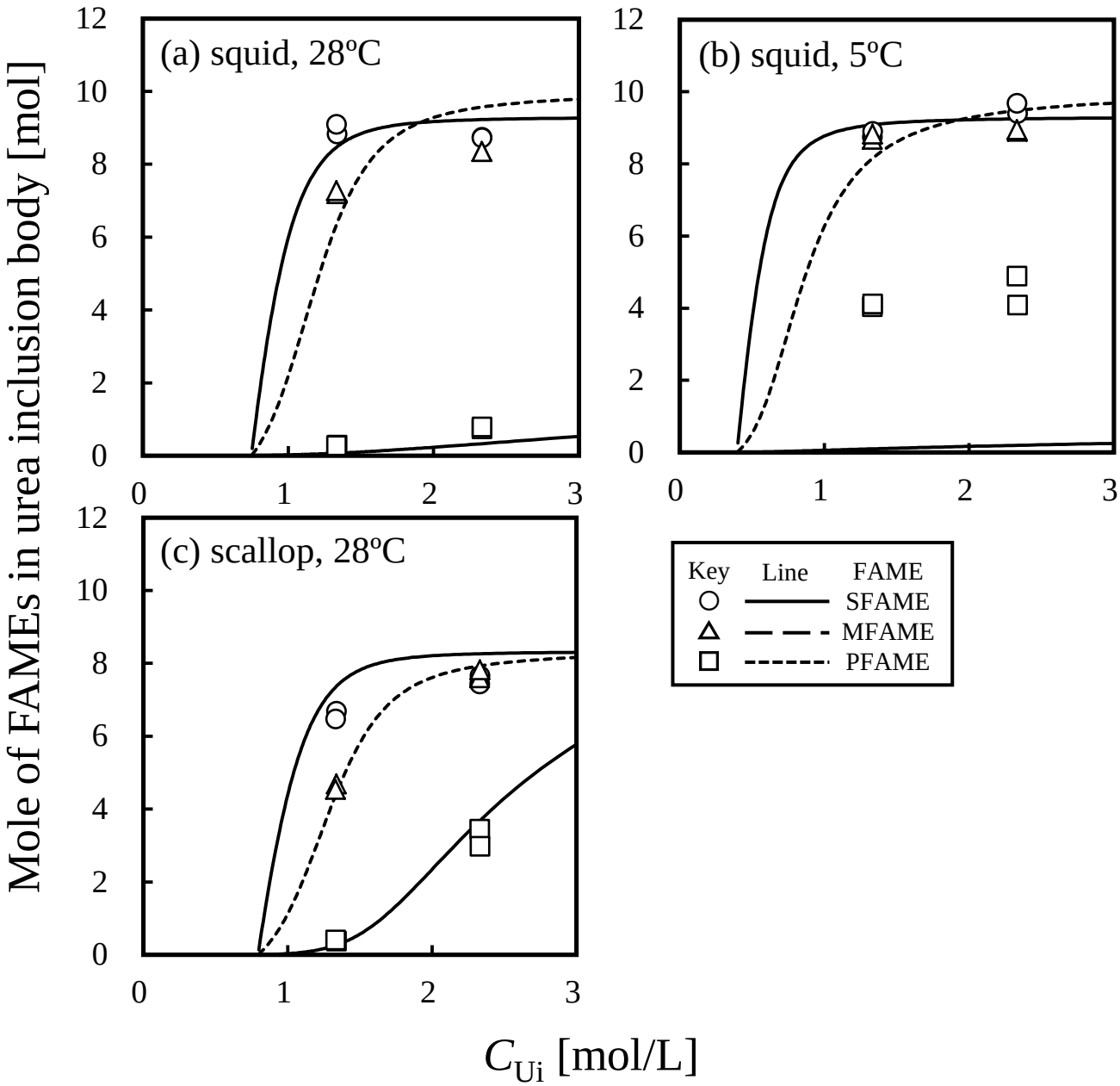

Fig. 13. Comparison between the molar amount of FAME in the solid phase (urea inclusion body) of the calculated (lines) and the experimental values (symbol) for (a) FAME derived from squid liver (28ºC), (b) FAME derived from squid liver (5ºC), and (c) FAME derived from scallop mid-gut (28ºC).

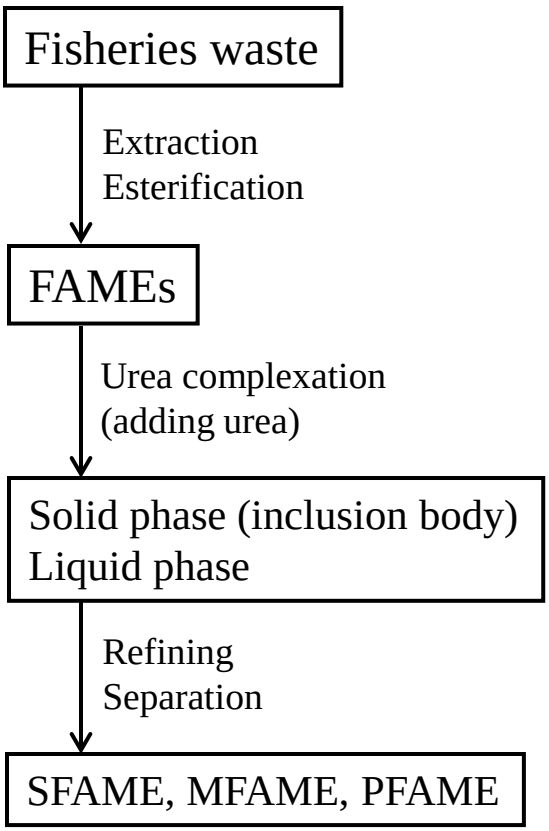

Fig. 14. Schematic diagram of process flow including urea complexation

Table 1

The contents of fatty acid derived from squid liver and scallop viscera.

Fatty Acid Methyl Ester		M.W. [g/mol]	Content [%]	
group	substance name		Squid	Scallop
S	Myristic Acid (C14:0)	242.40	3.56	3.69
M	Myristoleic Acid (C14:1n5)	240.40	0.20	0.64
S	Pentadecanoic Acid (C15:0)	256.43	0.14	0.12
M	cis-10-Pentadecanoic Acid (C15:1n5)	254.41	0.07	-
S	Palmitic Acid (C16:0)	270.46	17.3	17.6
M	Palmitoleic Acid (C16:1n7)	268.43	3.75	11.0
S	Heptadecanoic Acid (C17:0)	284.48	0.82	0.09
M	cis-10-Heptadecanoic Acid (C17:1n7)	282.46	1.16	0.52
S	Stearic Acid (C18:0)	298.51	4.32	2.94
M	Oleic Acid (C18:1n9c)	296.50	10.9	5.49
M	cis-11-Octadecenoic Acid (C18:1n7c)	296.50	3.64	6.06
P	Linoleic Acid (C18:2n6c)	294.48	0.82	1.68
P	Linolenic Acid (C18:3n3)	292.46	0.48	1.10
P	cis-6,9,12,15-Octadecatetraenoic Acid (C18:4n3)	276.41	0.60	2.29
M	cis-9-Eicosenoic Acid (C20:1n11)	324.54	3.80	1.06
M	cis-11-Eicosenoic Acid (C20:1n9)	324.54	3.28	1.29
P	cis-11,14-Eicosenoic Acid (C20:2n6)	322.53	0.49	0.35
P	Arachidonic Acid (C20:4n6)	318.50	1.97	2.26
P	cis-11,14,17-Eicosadienoic Acid (C20:3n3)	322.53	0.52	0.64
P	cis-5,8,11,14,17-Eicosapentaenoic Acid (C20:5n3)	316.48	10.2	22.7
M	cis-11-Docasenoic Acid (C22:1n11,13)	352.60	4.02	-
P	cis-13,16-Docosadienoic Acid (C22:2n6)	350.58	-	0.63
P	cis-7,10,13,16,19-Docosapentaenoic Acid Methyl Ester (C22:5n3)	344.53	1.05	0.35
P	cis-4,7,10,13,16,19-Docosahexaenoic Acid (C22:6n3)	342.51	18.2	8.58
	other		8.52	8.84

Table 2 The experimental condition of Figs. 3-6.

	material of FAME	mass of FAME [g]	initial urea concentration [mol/L]	volume of solvent [mL]	cooling temperature [℃]
Fig. 3	squid liver	0.25 ,0.50 ,0.75	1.33-2.33	5	28
Fig. 4	squid liver	1.0 ,2.0	1.33-2.33	10	28
Fig. 5	squid liver	0.25 ,0.50 ,0.75	0.62-2.33	5	5
Fig. 6	scallop midgut gland	0.25 ,0.50 ,0.75	1.33-2.33	5	28

Table 3 Model parameters determined from fitting of the data of Figs. 3-8 to Eq. (22) by a least squares method.

material of FAME	complexation temperature [°C]	x	n_1	n_2	n_3	m	K_1	K_2	K_3	K_4
squid liver	5	2.59	5.84	6.44	2.30	5.2	4219	1073	7.94×10^{-3}	13.9
squid liver	28	2.59	5.84	6.44	2.30	5.0	106	32.2	2.67×10^{-3}	0.44
scallop midgut gland	28	2.60	5.34	6.04	5.50	5.0	98.2	22.2	0.199	0.31

Table 4 Correlation coefficients, *r*, in determining model parameters by least squares method in Figs. 9-11.

	FAME [g]	V_i [mL]	SFAME *r* [-]	MFAME *r* [-]	PFAME *r* [-]	urea *r* [-]
Fig. 9 squid, 28ºC	0.25	5	0.927	0.961	0.842	0.966
	0.5	5	0.901	0.965	0.164	0.949
	0.75	5	0.967	0.954	0.904	0.989
	1.0	10	0.966	0.976	0.760	0.990
	2.0	10	0.764	0.733	0.390	0.978
Fig. 10 squid, 5ºC	0.25	5	0.998	0.988	0.976	0.966
	0.5	5	0.978	0.648	0.404	0.978
	0.75	5	0.985	0.992	0.735	0.983
Fig. 11 scallop, 28ºC	0.25	5	0.875	0.929	0.940	0.864
	0.5	5	0.967	0.922	0.836	0.992
	0.75	5	0.985	0.957	0.769	0.956